Early 2022 breakthrough infection sera from India target the conserved cryptic class 5 epitope to counteract immune escape by SARS-CoV-2 variants

Indrani Das Jana[1], Kawkab Kanjo[2], Subhanita Roy[1], Munmun Bhasin[2], Shatarupa Bhattacharya[5], Indranath Banerjee[3], Subhasis Jana[6], Arjun Chatterjee[7], Alok Chakraborty[8], Suman Chakraborty[4], Budhaditya Mukherjee[5], Raghavan Varadarajan[2*], Arindam Mondal[1*]

[1]Department of Bioscience and Biotechnology, Indian Institute of Technology Kharagpur, Kharagpur-721302, India
[2]Molecular Biophysics Unit (MBU), Indian Institute of Science, Bengaluru-560012, India
[3]B.C. Roy Technology Hospital, Indian Institute of Technology Kharagpur, Kharagpur-721302, India
[4]Department of Mechanical Engineering, Indian Institute of Technology Kharagpur, Kharagpur-721302, India
[5]School of Medical Science and Technology, Indian Institute of Technology Kharagpur, Kharagpur-721302, India
[6]Purba Medinipur District Hospital, Tamluk-721636, India
[7]Institute of Neuroscience, Kolkata-700017
[8]ICMR-National Institute of Cholera and Enteric Diseases, Kolkata-700010, India
[9]Lead contact: Arindam Mondal

Correspondence*: varadar@iisc.ac.in (R.V.), arindam.mondal@iitkgp.ac.in (A.M.)

Summary:

During the COVID-19 pandemic, the vast majority of epitope mapping studies have focused on sera from mRNA-vaccinated populations from high-income countries. In contrast, here we report an analysis of 164 serum samples isolated from breakthrough infection patients in India during early 2022 who received two doses of the ChAdOx viral vector vaccine. Sera were screened for neutralization breadth and potency against wildtype, Delta, and Omicron BA.1 viruses amongst which three were shortlisted for epitope mapping using charged scanning mutagenesis. These sera majorly targeted the recently identified class 5 cryptic epitope which is completely conserved across all SARS-CoV-2 variants and for different Sarbecoviruses. Consistent with these results, the sera show broad neutralizing activity against recent Omicron subvariants including XBB.1.5. Our study demonstrates that two vaccinations with the ChAdOx vaccine in a highly exposed population are sufficient to drive substantial neutralization breadth against emerging and future SARS-CoV-2 variants of concern.

Key Words: SARS-CoV-2, spike protein RBD, epitope mapping, breakthrough infection, convalescent serum, yeast display library, neutralizing antibodies, class-5/ RBD8 epitopes, immune escape, Omicron subvariant-XBB.1.5.

Introduction

Severe Acute Respiratory Syndrome Coronavirus 2 (SARS-CoV-2) has been circulating in the human population for over four years and rapidly evolving, causing the emergence of more than 50 different variants to date [1]. Multiple waves of infections were caused by the new variants despite massive vaccination programs, and their emergence was largely driven by the host immunity generated through natural infections and vaccination [2]. Detailed molecular-level understanding of the humoral immunity conferred by different vaccination regimens coupled with ongoing viral exposures is important both for the development of effective countermeasures against the current and future variants of SARS-CoV-2 and other Sarbecoviruses that may emerge in future.

More than 5.55 billion people, 72.3% of the world population, have received a single dose of COVID-19 vaccine [3], though in Africa, this number is less than 40% [4]. India ranks second highest after China in the number of COVID-19 vaccine doses administered (2.2 billion doses) [5]. The vaccination drive started in India on 16th January 2021, at the end of the first wave of infections caused mainly by the circulating B.1.1.7 (Alpha) and B.1.135 (Beta) variants. While the vaccination program was ongoing, the highly infectious B.1.617.2 (Delta) variant emerged and caused the second wave of the pandemic (March to October 2021), which resulted in the highest number of daily infections with high disease severity and mortality rate [6,7]. By January 2022, more than 77% of the Indian population were immunized; the new highly transmissible and heavily mutated B.1.1.529 (Omicron) variant emerged and led to the third wave of infection but was associated with milder symptoms and lower fatality rates [8]. A significant fraction of the vaccinated population in India got infected during the second and

67 third waves of the pandemic, leading to the large number of “breakthrough infections” [9]. These
68 breakthrough infections shaped the transmission dynamics and contributed to the overall
69 evolution of the virus [10]. After 2021, there was little vaccine uptake in the country and the
70 percentage of the population that received a third (booster) dose was only about 10%.

71 The SARS-CoV-2 spike protein (S) is the main surface glycoprotein that mediates the
72 interaction with the host angiotensin-converting enzyme 2 (ACE2) receptor and subsequent
73 fusion of the viral envelope with the host cell membrane that marks the initiation of the
74 infectious cycle [11,12]. The S protein is the primary target for neutralizing antibodies elicited
75 through natural infection as well as vaccination [13–15]. The spike constitutes a trimer where
76 individual protomers are comprised of two subunits, S1 and S2 [16]. S1 harbours the N-terminal
77 domain (NTD), the Receptor Binding Domain (RBD), and the S2 houses the fusion peptide,
78 the heptad repeats 1 and 2 (HR1, HR2), the transmembrane domain (TM) and the C-terminal
79 domain (CD). The majority of human neutralizing antibodies, isolated from convalescent or
80 vaccinated sera, target conformational epitopes in the RBD Receptor Binding Motif (RBM) or
81 in the conserved core of RBD[17–19] . In the context of the spike trimer, the individual RBDs can
82 be either in the up or down conformation, with only the former able to bind the ACE2 receptor.

83 The epitopes targeted by neutralizing antibodies can be classified into four major
84 classes (Class 1-4) [20]. Class 1 and class 2 epitopes overlap with the ACE2 binding site, and
85 antibodies targeting these sites competitively inhibit receptor binding. While class 1 epitopes
86 are accessible when RBD is present in the up conformation, class 2 epitopes are accessible
87 in both up and down conformations [21]. For certain class 2 epitope targeting antibodies (C144),
88 the long complementary determining region (CDR) of the heavy chain acts as a bridge
89 between adjacent RBDs from neighbouring protomers in the down conformation, thus locking
90 the S trimer into the prefusion closed conformation; an unusual mode of neutralization [21]. In
91 general, the antibodies targeting class 1 and class 2 epitopes have strong neutralizing activity.
92 However, different SARS-CoV-2 variants escape neutralization by these antibodies by
93 acquiring mutations in the RBM region that is part of the class 1 and 2 epitopes, compromising
94 their efficacy. Both class 3 and class 4 antibodies bind to the RBD core region away from the

95 ACE2 binding site. N343 glycan and the surrounding residues are accommodated in class 3
96 epitopes [22]. S309 antibody, a class 3 antibody isolated from a SARS-CoV infected individual,
97 exhibited broad cross-reactivity against SARS-CoV and SARS-CoV-2, although many SARS-
98 CoV-2 VOCs acquired mutations in class 3 epitopes to escape neutralization by these
99 antibodies [21]. The cryptic epitope around the RBD base (first described for CR3022 antibody)
100 constitutes the highly conserved class 4 epitope and is accessible only in the RBD up
101 conformation[23–26]. Despite their rare prevalence in convalescent sera, antibodies targeting
102 class 4 epitopes are suggested to protect against emerging VOCs and other sarbecoviruses.
103 Additionally, a highly conserved class 5 epitope has been recently identified and characterized
104 as a target for broadly neutralizing antibodies [27,28].
105
106 Mapping monoclonal antibody epitopes can inform about viral evolution and aid in the
107 development of epitope-based vaccines and therapeutics. However, mapping conformational
108 epitopes targeted by polyclonal sera remains challenging. Mapping these epitopes can
109 elucidate how escape mutations in the viral antigen impact the neutralization potency of the
110 human polyclonal sera harbouring a heterogeneous mixture of antibodies. In the present
111 study, we have conducted a comprehensive analysis of human sera collected from individuals
112 vaccinated with two doses of the ChAdOx1 nCoV-19 viral vectored vaccine and subsequently
113 had undergone breakthrough infections. Neutralization efficacies of 164 sera samples were
114 screened against SARS-CoV-2 pseudoviruses representing the parental strain WA.1 or VOCs
115 B.1.617.1, B.1.617.2 and B.1.1.529. Nine individuals whose serum samples exhibited broader
116 neutralization were subjected to longitudinal sampling and three of them were shortlisted for
117 epitope mapping. Utilizing charge scanning mutagenesis [29,30], a library of individual charged
118 substitutions at all the solvent-exposed positions of the wild-type RBD was generated and
119 displayed on the yeast surfaces to map the epitopes targeted by the polyclonal sera. A high
120 fraction of antibodies targeting either class 1 epitopes or the rare cryptic class 5 epitope, also
121 denoted as RBD8 [43], were observed in all three sera tested. The class 5/ RBD8 epitope
122 residues identified in this study are highly conserved across all SARS-CoV-2 variants,

consistent with the observed neutralizing potency of the selected serum samples against heavily mutated Omicron BA.1, BA.5, and the recent XBB.1.5 variant. Our findings illustrate how a combination of vaccinated and breakthrough infections in a highly exposed population can elicit diverse antibody classes that confer potent neutralizing activity with broad cross-reactivity, providing insights into why deaths and hospitalizations have remained low post-2021 in virtually all low and middle-income countries (LMICs) even in the absence of variant updated vaccine boosters.

Results

Study cohort

In contrast to vaccination alone, hybrid immunity resulting from SARS-CoV-2 breakthrough infections has been shown to boost neutralizing antibody titers while increasing their breadth at the same time[31,32]. We shortlisted individuals who received two doses of the ChAdOx1 nCoV-19 viral vector vaccine between April and November 2021 and then were infected between November 2021 and January 2022, which marks the transition between the second and third waves of the pandemic, in India caused by the B.1.617.2 (Delta) and B.1.1.529 (Omicron) variants, respectively [33]. We hypothesized that such individuals would have developed broadly cross-reactive neutralizing antibodies that are effective against different variants of concern [31,32]. Blood samples, along with questionnaires about gender, age and symptoms, were collected from 164 shortlisted individuals who were voluntarily recruited by a separate consent for this study. All participants were confirmed positive by RT-PCR for SARS-CoV-2 infection during the abovementioned time frame, which is within 2-4 months post-second dose of vaccination (Figure 1A, B). The serum samples were collected from the individuals within 4-6 weeks of their breakthrough infection. The study cohort consisted of 90 males and 74 females; the median age was 36 and 34 years, respectively (Figure 1D). Most

150 volunteers showed mild symptoms with 5.84% (10 individuals) population showing severe to
151 critical illness.
152
153 **Neutralization profile of the polyclonal serum samples against SARS-CoV-2 variants.**

154 We employed a high throughput neutralization assay based on reporter lentiviruses
155 pseudotyped with spike proteins from SARS-CoV-2 parental WA.1, B.1.617.1 (Kappa),
156 B.1.617.2 (Delta) and B.1.1.529 (Omicron) strains [34]. These pseudoviruses were incubated
157 with dilutions of serum samples ranging from 10^{-2} to 10^{-4} before infecting HEK-293T cells
158 overexpressing ACE2. The reporter signal was measured as a proxy of the infectivity, which
159 was the highest for the mock-treated cells and the lowest for a polyclonal antibody preparation
160 that binds the spike protein and has high neutralization activity (Novus Biologicals, NB100-
161 56578). The neutralization efficacies of 164 serum samples against WA.1 and different VOCs
162 was represented as a heatmap with colours ranging from red (high neutralization) to green
163 (low neutralization) (Figure 1C). Overall, the serum samples from this study exhibited
164 maximum neutralizing activity towards the Delta variant followed by the Kappa variant with a
165 geometric mean (GM) of 93% and 90%, respectively (Figure 1E). Reduced neutralizing activity
166 was observed against the parental WA.1 strain (GM-73%), which was further lowered against
167 the Omicron variant (GM-46%) (Figure 1E). These results suggest that majority of the
168 individuals in the study cohort had breakthrough infections caused by the Delta variant. Most
169 of the serum samples neutralized Delta and Kappa variants better than WA.1 (Figure 1C,
170 heatmap) due to the high similarity between the spikes of both variants [35]. Interestingly, certain
171 sera (BCRTH 29, 30, 33, 35, 45, 46) showed potent neutralization against WA.1 but failed to
172 neutralize other tested VOCs, especially at higher dilutions (Figure 1C). This suggests that
173 vaccination and subsequent infections have primed a strong immune response towards the
174 parental strain but failed to generate antibodies that are broadly cross reactive against the
175 VOCs, as also reported previously[36]. A few serum samples showed high neutralization activity
176 against the Omicron variant (Figure 1C). Limited neutralization activity against the heavily

177 mutated Omicron variant results from the high number of mutations conferring extensive
178 immune escape from vaccine and infection sera [37].

179 **The breadth and cross-reactivity of the shortlisted polyclonal serum.**

180

181 Serum samples with broadly cross-reactive neutralizing activity against WA.1, Kappa,
182 Delta and Omicron variants at 10^{-2} dilution were selected for further studies. Out of 164 serum
183 samples, 29 (17%) showed more than 65% neutralization against all four VOCs (Figure 1F &
184 Figure 1C, red diamonds) and hence, were considered as broadly neutralizing serum samples.
185 We selected 9 volunteers who have not been infected and had not received any vaccine
186 booster post the first round of blood collection and obtained their consent to participate in a
187 second round of blood sampling. The second set of serum samples (late) was collected from
188 the 9 selected individuals 4-6 weeks post the first set (early), and both early and late sets of
189 serum samples were subjected to further analysis.

190

191 Neutralization efficacies of the shortlisted serum samples were determined against
192 WA.1, Delta and the Omicron variants using the pseudovirus neutralization assay (Figure S1)
193 and neutralization titers were represented in the form of IC_{50} (Figure 2A, B, Early). Amongst
194 the nine serum samples collected at the early time point, four showed the highest IC_{50} values
195 for Delta, three for the parental WA.1 strain and two for the Omicron; a trend that matched
196 with the overall neutralizing activity of the larger cohort of 164 samples (Delta> WA.1>
197 Omicron; Figure 1E). Interestingly, this was not the case for the serum samples collected from
198 the same volunteers at the later time point (Figure S1 and Figure 2A, B Late). A moderate to
199 sharp decline in neutralizing activity (2-18 fold change in IC_{50}) was observed for most serum
200 samples between early and late time points (Figure 2 C, D). Interestingly, a few sera had an
201 increase or maintained similar variant-specific neutralization titers at both time points.
202 Compared to the early time point neutralization profile, BCRTH01 and INK41 showed a
203 significant decline in neutralization titer against WA.1 but a slight increase in neutralization
204 titer against the Omicron variant, at the late time point. This may reflect the higher durability

205 of the variant specific (Omicron or Delta) antibodies generated by the breakthrough infections
206 with respect to the parental strain (WA.1) specific antibodies elicited through vaccination.
207 Interestingly, BCRTH01, INK09, INK36 and INK41 sera maintained high neutralization titers
208 against all the pseudoviruses tested and at both time points, with INK36 being the most potent
209 neutralizing sera.
210
211 As the majority of the neutralizing antibodies target the receptor binding domain (RBD)
212 of the spike protein [17–19], we sought to test the binding activity of the four serum samples
213 (BCRTH01, INK09, INK36 and INK41) to the spike RBD. Enzyme-linked immunosorbent
214 assay (ELISA) was performed with recombinant purified spike RBD derived from the WA.1,
215 Omicron BA.1 and BA.5, which are used as coating antigens. As expected, all four serum
216 samples bound well to the RBD variants, indicating high abundance of RBD-targeted
217 antibodies in them (Figure S2 A). All sera samples showed highest IgG titres against WA.1
218 and marginally lower titres against BA.1 and BA.5 (2.2– 4.8 fold reduction) (Figure S2 B, C),
219 except for INK41, which showed 9.1 fold reduction for BA.1 compared to the WA.1. BA.5 RBD
220 exhibited higher sensitivity than BA.1, but lower sensitivity than WA.1 for binding to all four
221 serum samples tested. Three serum samples with high neutralizing activity against different
222 variants of SARS-CoV-2, namely BCRTH01, INK09 and INK36, were selected for further
223 studies.
224
225 **Comprehensive mapping of RBD epitopes targeted by the shortlisted human serum.**
226 We employed a charged scanning mutagenesis library of SARS-CoV-2 RBD displayed at the
227 yeast surface as a novel approach to identify the epitopes targeted by the antibodies present
228 in the polyclonal serum samples (Figure 3A). WA.1 RBD (332-532) was used as the template
229 for library construction and all RBD residues with solvent accessibility >15% were individually
230 mutated to negatively charged Aspartate, with the exception of negatively charged residues,
231 which were mutated to the positively charged Arginine. The generated RBD library was
232 displayed on the yeast surface and subjected to binding with a saturating concentration of the

233 polyclonal serum sample as determined by sera titration on the yeast surface (Figure S3 A).
234 Binding was detected using fluorescently labelled antibodies, and the yeast cell populations
235 were sorted into different bins through Fluorescence Activated Cell Sorting (FACS) (Figure S3
236 B-D). Yeast populations within these bins were subjected to deep sequencing to identify the
237 mutations responsible for abolishing binding to the serum. The deep sequencing reads were
238 analyzed as described in the methods section. Briefly, the binding and expression signals of
239 each mutant RBD were normalized with respect to the wildtype and the MFI ratio between the
240 normalized Mean Fluorescence Intensities for expression (MFI-expression) and binding (MFI-
241 binding) for each of the RBD variants was calculated.
242
243 Epitope mapping was performed with all three of the shortlisted serum samples
244 (BCRTH01, INK09 or INK36) and RBD residues whose mutation resulted in MFI_{Ratio} one
245 standard deviation higher than the mean MFI_{Ratio} were considered epitopes (Figure 3B, Table
246 S2). A high value of MFI_{Ratio} (darker shades of red) indicates that the charged substitution
247 significantly perturbed the binding of the serum samples with minimum or no effect on
248 expression. The MFI_{Ratio} of the identified epitope residues were mapped on the RBD structure
249 (Figure 3C). Overall, the identified epitopes (highlighted in lighter to dark shades of red) for all
250 three serum samples were clustered in two major groups; (i) epitopes that overlap with the
251 ACE2 binding motif (RBM) and (ii) epitopes that are away from the RBM. Interestingly, for
252 BCRTH01 serum, an enrichment in non-RBM over RBM epitope residues was observed.
253 However, this was not the case for INK36 or INK09, where epitope residues across different
254 RBD regions were enriched to similar levels.
255
256 To validate the results of the yeast-display screening and deep sequencing, we
257 selected three RBD residues identified as an epitope and another three residues identified as
258 non-epitope residues in the context of BCRTH01 serum and reintroduced these mutations to
259 the RBD individually followed by yeast surface display and BCRTH01 binding evaluation via
260 flow cytometry (Figure 3D). We selected the non-RBM epitope residues (T430, T437 and

261 R466) as they showed high values of MFI_{Ratio} compared to the wildtype. As shown in Figure
262 3D, charged substitution at the putative epitope residues significantly impacted the binding to
263 the serum while charged substitution at putative non-epitope residues had minimum or no
264 effect upon the binding (Figure S4 A, B & Figure 3D). This data validates the epitope residues
265 identified through the current study and establishes the robustness of the charged scanning
266 mutagenesis approach for the identification of epitope residues targeted by polyclonal human
267 serum.
268
269 **Antibodies in the shortlisted sera target a cryptic epitope that is broadly conserved**
270 **across different SARS-CoV-2 variants.**

271 Previous epitope mapping studies on convalescent polyclonal serum samples showed
272 enrichment of antibodies targeting the class-1, -2 and -3 epitopes and to a lesser extent the
273 class-4 epitope [37–41]. Hence, we analysed the different epitopes identified in the present study
274 and compared them to the epitopes reported in the literature. The major neutralizing epitopes
275 in the RBD are categorized into four major classes, class 1-4 (Figure 4 and Table S1). Out of
276 the 26 epitopes residues identified, eight were classified as Class 1, two as Class 2, two as
277 Class 3 and five as Class 4. Surprisingly, 11 out of the 26 (42%) epitope residues do not belong
278 to any of these major classes (except for K356 which is shared with class 3 and T470 which
279 is shared with class 2), but instead belong to a rare cryptic epitope [42,78], situated away from
280 the receptor binding motif of RBD (Figure 4A).

281 Residues constituting the cryptic epitope were recently designated as class 5 [27] or RBD8
282 class of epitope [43] (Figure S5). This rare cryptic epitope spans diagonally across the base of
283 the RBD (Figure 4A, S5) and is situated on the opposite surface of the ACE2 binding motif,
284 thereby remain buried and inaccessible in the prefusion closed conformation of the Spike
285 trimer (Figure 4B). Hence, binding of class 5 antibodies, such as BIOLS56, IMCAS74, WRAIR-
286 2063/ S2H97/ WRAIR-2057/ WRAIR-2134, to this rare cryptic epitope requires extensive
287 opening of the pre-fusion structure, thereby inducing rapid and premature transition to the

288 post-fusion conformation and S1 shedding [27,43–45]. These antibodies cross-reacted with all
289 SARS-CoV-2 VOCs, including Delta, Omicron BA.4/BA.5, BQ.1.1, and the recent highly
290 immune escaping variant XBB1[43,44]. Supporting this notion, class 5 epitope residues identified
291 in our analysis were highly conserved not only across all the different SARS-CoV-2 VOCs
292 (Figure 4C) but also across different Sarbecoviruses (Figure S6). Interestingly, the BCRTH01
293 serum had the highest number (total 10) of class 5 identified epitope residues compared to
294 the INK09 and INK36 (7 and 8 residues, respectively) (Figure 4A, Table S1), which explains
295 its breadth and high cross-reactivity against the different SARS-CoV-2 variants tested. In
296 contrast, INK36 has the highest number of class 1 and class 2 epitopes (8 and 2, respectively)
297 that are targeted by ACE2 competing antibodies, consistent with its highest neutralization
298 activity amongst the three shortlisted serum samples.

299 To evaluate the effect of charged substitutions on neutralizing activity of the polyclonal
300 sera, we selected four of the RBD-identified epitope residues and individually mutated them
301 to charged substitutions in the WA.1 backbone. This is followed by generation of
302 pseudoviruses harbouring these mutant spike proteins. Two mutations, R403D and G416D,
303 are situated within the RBM and are expected to perturb class 1 or class 1/ 4 epitope-specific
304 antibodies, respectively while the other two mutations, T430D and R466D, are situated away
305 from the RBM. T430D is expected to interfere with the binding of class 4 and class 5/ RBD8
306 epitope-specific antibodies, while R466D is expected to disturb the latter (Figure 4, Table S1).
307

308 We tested the sensitivity of WT and mutant pseudoviruses to neutralization by BCRTH01
309 serum. As expected (Figure 5 A, B), all the mutations reduced the neutralization activity of the
310 polyclonal serum in comparison to the WT pseudovirus, with R466D and R403D mutants
311 showing 132-fold and 48.9-fold reduction in the neutralization titer (IC_{50}), respectively. In
312 contrast, T430D and G416D mutations showed moderate and comparable effects with 3.55-
313 and 4.12-fold reduction in IC_{50} values, respectively. Together, our data suggests that the
314 polyclonal serum (BCRTH01) used in this study harbours the highest fraction of class 5/ RBD8
315 and class 1 antibodies, and a lower fraction of class 4 antibodies. This combination of ACE2

316 competing (class 1) and non-competing (class 5/ RBD8 and class 4) antibodies imparts high
317 neutralization efficacy and broad cross reactivity to these serum samples, which render it
318 effective against different variants of SARS-CoV-2, including the currently circulating ones.

319 **Pre-XBB serum neutralizes the recent Omicron subvariant XBB.1.5.**

320 The heavily mutated Omicron subvariant, XBB and XBB.1, emerged in late 2022 and
321 soon, XBB and its descendants accounted for the majority of infections in the whole world [46,47].
322 The variant XBB.1.5 harbors a rare mutation, F486P, which demonstrates superior
323 transmissibility and immune escape towards vaccines and monoclonal antibodies, accounting
324 for its rapid spread in more than 100 counties [48–53]. Interestingly, the epitopes identified in this
325 study remain completely conserved for XBB.1.5 (Figure 4C), suggesting that the shortlisted
326 serum samples should neutralize this recent subvariant of SARS-CoV-2. Thus, we generated
327 pseudoviruses harboring either WA.1, Omicron BA.1 or Omicron XBB.1.5 spike proteins at
328 their surface and performed neutralization assays with the shortlisted serum samples
329 (collected in early 2022, well before the emergence of XBB). As expected (Figure 5 C-F), all
330 three serum samples showed neutralizing activities against Omicron BA.1 and XBB.1.5
331 comparable to the parental WA.1 strain, specifically for INK36 and INK09 serum. For
332 BCRTH01, the neutralizing activity towards the XBB.1.5 is comparable to that of the Omicron
333 BA.1 but 2.7 fold lower than for WA.1. This indicates that the shortlisted volunteers, who had
334 breakthrough infections following vaccination during the Delta/ Omicron wave (December
335 2021) of the pandemic, generated humoral immunity that remained effective even against
336 recently emerged subvariants (February-March 2023). This, in turn, establishes the potential
337 importance of the identified epitopes as a target for developing vaccine candidates against
338 future SARS-CoV-2 variants.

339

340 **Discussion.**

341 Breakthrough infections caused by waning immunity to SARS-CoV-2 VOCs have been
342 reported to induce enduring humoral immunity and generate broadly neutralizing antibodies
343 capable of combating different SARS-CoV-2 variants as well as SARS-CoV and other
344 Sarbecoviruses [32,54,55]. Human high-resolution epitope mapping studies following vaccination
345 and/or infection have been largely focused on sera from US or European populations that
346 were primarily immunized with mRNA vaccines [19,41,59,61] while a few studies focused on sera
347 from individuals vaccinated with CoronaVac whole virus inactivated vaccine with or without
348 breakthrough infection [52,63,65]. Little is known about the humoral response in LMICs and China,
349 which are home to ~85% of the world's population. In the present study, we describe epitope
350 mapping studies of sera from an Indian population of individuals who received two doses of
351 viral vectored vaccine followed by "breakthrough infections" within 4-6 weeks post-second
352 dose. The timing of the study was deliberately chosen at the intersection of the second and
353 third waves of the pandemic instigated by B.1.617.2 and B1.1.529, which, in theory, is
354 expected to enhance the breadth and potency of antibodies generated through vaccination
355 (parental strain WA.1) and subsequent infections by different VOCs[32]. Around 18% of the
356 serum samples exhibited > 65% neutralizing activity against the parental strain and different
357 VOCs including Kappa, Delta, and Omicron. Furthermore, via longitudinal sampling, three
358 serum samples were identified that not only maintained their broad neutralizing activity up to
359 12 weeks post-infection but also demonstrated effectiveness against the recent circulating
360 Omicron subvariant XBB.1.5. Although prior exposure to Omicron spike, including BA.1
361 bivalent vaccination was reported to generate XBB.1.5 specific antibodies [56], the neutralizing
362 activity remains low compared to the parental WA.1 or D614G strains [50,56–58]. Several studies
363 have demonstrated a substantial escape of XBB variants from neutralization by convalescent
364 and vaccinated sera, with more than 20-fold reduction in neutralization titres compared to
365 WA.1 [39,52,57,67]. Strikingly, the shortlisted serum samples used in this study showed less than
366 3-fold decrease in neutralizing titers against Omicron BA.1 and XBB.1.5 compared to the
367 parental strain, hence representing proof towards the role of hybrid immunity in generating
368 highly potent, durable, and broadly cross-reactive neutralizing antibodies.

369 We employed an aspartate scanning mutagenesis and yeast surface display coupled
370 with flow cytometry and deep sequencing to map epitope residues which, upon charged
371 substitution, severely impacted the binding of the serum antibodies without affecting the
372 expression. Charge scanning mutagenesis has been previously proven to be effective in
373 identifying residues buried at protein-protein interaction interface [60,62]. While Deep Mutational
374 Scanning using yeast surface display has been previously employed to identify serum escape
375 mutations on SARS-CoV-2 RBD [19,64], the relatively smaller size of the aspartate scanning
376 library, together with the unique barcoding strategy of the individual mutant ORFs employed
377 by us simplify library construction and downstream analysis. Using this method, we identified
378 a total of 26 surface-exposed amino acid residues whose mutation significantly impacted the
379 binding of the polyclonal sera and, hence, are designated as potential epitopes targeted by
380 the sera. The majority of these residues have been previously identified as part of epitopes for
381 different classes of RBD neutralizing monoclonal antibodies [66], thus supporting the robustness
382 of the novel screening approach in identifying epitopes targeted by polyclonal sera.

383 The epitopes identified using the proposed analysis can be broadly categorized into
384 two main groups: RBM epitopes overlapping with the ACE2 binding motif and non-RBM
385 epitopes. The RBM epitopes consist primarily of class 1 and class 2 epitopes which are
386 targeted by antibodies that competitively hinder receptor engagement and virus attachment to
387 host cells. While antibodies targeting these epitopes are responsible for the high neutralizing
388 activity of polyclonal serum used in this study [17,21,68–70], these regions are heavily mutated in
389 emerging VOCs, thereby limiting the breath and cross-reactivity of antibodies targeting these
390 epitopes [25,26,45,71]. For example, the R403K mutation, in the class 1 epitope, has been classified
391 as “vaccine escape mutation”, leading to higher infectivity and lower neutralizing activity of
392 vaccine-elicited antibodies against the recent JN.1 subvariant of Omicron [72]. Interestingly, the
393 R403D mutation resulted in 48.9 fold reduction in neutralizing activity of the BCRTH01 serum
394 as evidenced in our study. Another identified class 2 epitope residue substitution L452R, was
395 associated with a massive expansion and immune escape of the Delta variant from vaccine-
396 elicited class1 and class 2 antibodies[41] during the second year of the pandemic [73]. Similarly,

397 the F456L mutation (class 1 epitope) is associated with heightened ACE2 binding, infectivity,
398 and immune evasion from the XBB.1.5 neutralizing antibodies [74] leading to the global spread
399 of EG.5 (Eris) subvariant [75] in the recent past. The K356T mutation in JN.1, in the class 3
400 epitope, drives resistance towards Sotrovimab, a class 3 antibody (S309) based antiviral drug
401 [76]. In contrast to classes 1-3, the class 4 epitopes targeted by the shortlisted sera described
402 above show high conservation (Figure 5B). These class 4 epitopes are situated in the RBD
403 core region, away from the RBM except for the G416, which resides within RBM. Class 4
404 antibodies targeting G416 (COVA1-16, C118 and C022) and surrounding residues sterically
405 hinder ACE2 binding [25,26] thereby resulted in high neutralizing activity.

406 A major fraction (11/26) of the epitope residues identified in the present study belong
407 to a rare cryptic epitope [42,77,78], rarely seen in the repertoire of antibodies from convalescent
408 sera [38–41]. Recently, this cryptic epitope has been categorized as class 5 or the RBD8 class of
409 epitopes [27,43]. These antibodies are reported to get enriched by breakthrough infections
410 caused by Omicron subvariants [52]. The amino acid residues constituting these epitopes are
411 clustered together at the opposite surface from the ACE2 binding motif of RBD and remain
412 inaccessible in the closed trimeric form of the spike (S) (Figure 4B, upper panel). Such
413 epitopes can only be accessible through breathing of the prefusion structure of the trimeric S
414 protein (Figure 4B, upper panel) whereby antibody binding ultimately leads to shedding of the
415 S1 subunit [43]. Additionally, it has been proposed that the binding of class 5 antibodies leads
416 to premature, receptor-independent conversion of S from pre to post-fusion conformation,
417 ultimately blocking viral entry and syncytium formation [79]. Interestingly, class 5 epitope
418 residues remain completely conserved across all SARS-CoV-2 variants and for different
419 Sarbecoviruses, indicating the cross-reactivity and increased breadth of class 5 antibodies
420 against these viruses. Consistent with this, the shortlisted serum samples, enriched for RBD8
421 epitope antibodies, effectively neutralized WA.1, Delta, Kappa, Omicron BA.1 and XBB.1.5.

422 Lately, antibodies targeting non-RBM epitopes in the spike protein have emerged as
423 prime candidates for developing broad-spectrum vaccines or therapeutics against SARS-CoV-

424 2 variants [28,80,81]. Some of these antibodies showed cross reactivity against different
425 Sarbecoviruses, thus further extending the prophylactic/therapeutic potential of such
426 antibodies against future emerging SARS-like coronaviruses. However, non-RBM antibodies
427 are limited by their weak neutralization activity. Rao et al., have shown that the RBD8 antibody
428 (BIOLS56) can rescue the immune escape caused by an RBM targeting antibody (IMCAS-
429 L4.65), together ensuring strong neutralizing activity and broad neutralizing efficacy against
430 different Omicron variants [43]. In this study, we show that an immune response elicited by hybrid
431 immunity and containing a combination of class-1 (RBM targeting) and class 5/ RBD8
432 antibodies can achieve neutralization potencies against different SARS-CoV-2 variants
433 including WA.1, Kappa, Delta and multiple Omicron subvariants including the recent XBB.1.5.
434 Furthermore, mutation of a single class5/ RBD8 epitope residue (R466D) resulted in 132 fold
435 reduction in the neutralization titer which is even higher than that observed in the case of
436 mutations of class 1 (R403D) epitope (48.9 fold), suggesting high abundance and comparable
437 neutralization efficacy of these two different classes of antibodies (class 5/ RBD8 and class 1)
438 in the shortlisted serum samples. This contrasts with the previously conducted epitope
439 mapping studies from the convalescent polyclonal serum samples, which led to the
440 identification of class 1-4 epitope targeting antibodies [38–41].

441 In conclusion, antibodies targeting different classes of epitopes may synergistically
442 contribute to achieving high neutralizing activity (Class 1+2 epitopes) and broader cross-
443 reactivity (Class 4 and RBD8) against all variants of SARS-CoV-2. Notably, RBD8 constitutes
444 a significant portion of the epitopes identified in all three serum samples, which differs from
445 the typical composition of the convalescent serum samples analysed previously [38–41]. In India,
446 after the Delta wave in mid-2021, there was little masking or isolation, and likely continued
447 extensive viral exposure. This, coupled with the relatively young population (median age 28.4
448 years) may have contributed to the generation of broadly cross reactive antibodies targeting
449 novel cryptic epitope presented here. These findings need to be confirmed in larger epitope
450 mapping studies. Understanding this adaptive strategy implemented by the host could pave

451 the way for the development of universal vaccines and therapeutics against future SARS-CoV-
452 2 variants and future sarbecovirus outbreaks.

453

454 **Acknowledgement and Funding:**

455 A.M. acknowledges the Indian Council for Medical Research (VIR/COVID-19/19/2021/ECD-I)
456 and the Science and Engineering Research Board (SERB-DST (CRG/2022/003628) for
457 providing financial support. R.V. is a JC Bose Fellow of DST. This work was funded by a grant
458 from the Bill and Melinda Gates Foundation (INV-042471) to RV. Funding for infrastructural
459 support was from DST FIST, MHRD, and the DBT IISc Partnership Program. I.D.J.
460 acknowledges the Science and Engineering Research Board (SERB) for the National Post
461 Doctoral Fellowship (PDF/2023/000284) awarded to her. K.K. acknowledges the support of
462 an MHRD-IISc doctoral fellowship. The authors acknowledge project staff Shyamal Manna for
463 his support in blood collection. The funders had no role in study design, data collection and
464 interpretation, or the decision to submit the work for publication.

465 **Authors' Contributions:**

466 Conceptualization—A.M., and R.V. Designing experiments—A.M., R.V., I.D.J. and K.K.
467 Performing experiments—I.D.J., K.K., and S.R. Manuscript writing—A.M., R.V., I.D.J. and
468 K.K. Fund acquisition—A.M., R.V., B.M., and S.C. Manuscript editing— A.M., R.V., I.D.J. and
469 K.K, B.M., S.C. and A.C. Deep Sequencing reads processing—M.B., Medical supervisors in
470 cohort identification and blood collection—S.J., A.C., and I.B.

471 **Declaration of interests:** The authors declare no competing financial interests or dispute in
472 the relationships that could have appeared to influence the work reported in this article.

473

474 **Figure titles and legends**

475

476 **Figure 1. Study cohort and timeline.** (A) Schematic representation of study design. (B)
477 Distribution of the study cohort as a function of the timeline of vaccination and breakthrough
478 infection in the context of the second and third wave of pandemics caused by different VOCs
479 of SARS-CoV-2. Red bars indicate the time points of serum sample collection for the entire
480 cohort (early) and subsequently for the shortlisted individuals (late). (C) Heatmap of
481 neutralizing activity of the 164 serum samples (at dilutions; 0.01, 0.001, 0.001) against the
482 parental strain and different VOCs of SARS-CoV-2 with green to red representing the lowest
483 to highest extent of neutralization (%). (D) Age distribution of male and female volunteers
484 included in the study cohort. (E) Comparison of the relative neuralization efficacies of the
485 serum samples (at 0.01 dilution) against parental strain and different VOCs. (F) Venn diagram
486 showing cross-reactivity of the shortlisted serum samples displaying more than 65%
487 neutralization (at 0.01 dilution) towards at least one of the pseudoviral variants tested in this
488 study. A total of 29 serum samples with >65% cross-reactivity towards all the VOCs tested in
489 this study were designated as broadly cross-reactive sera (red diamonds in 1C).
490
491 **Figure 2. Neutralizing activity of the shortlisted serum samples collected at early and**
492 **late time points.** (A) Comparative analysis of the neutralization titers (IC_{50}) of serum samples
493 isolated from the shortlisted 9 volunteers during 1st (early) and 2nd (late) batches of sample
494 collection, against WA.1, B.1.617.2 and BA.1. (B) Heatmap showing fold change in the IC_{50}
495 values for B.1.617.2 and BA.1 with respect to the parental WA.1 strain with red to white
496 indicating higher to lower neutralization titers. (C) Comparative analysis of the pseudovirus
497 neutralization titers of the serum samples isolated at early and late time points. (D) Heatmap
498 representing variant-specific fold change in IC_{50} values.
499
500 **Figure 3. Epitope mapping through yeast display analysis.** (A) Schematic representation
501 of the yeast display screening as described in the text. (B) The heat map represents the ratio
502 of MFI-expression to MFI-binding extracted from deep sequencing reads analysis. The higher
503 to lower ratios are represented in a red to blue gradient. The higher the ratio (*Red*), the more

504 sera escape at that position. The RBM is demarcated on the structure using a black line. (C)
505 The MFI-expression/ MFI-binding ratios are mapped on the RBD structure (PDB ID: 6M0J)
506 following the same color scheme. (D) The ratio of MFI-expression to MFI-binding of WT and
507 mutant RBDs w.r.t BCRTH01 serum, harboring mutations at the epitope and non-epitope
508 residues, are presented.

509 **Figure 4.** (A) Individual epitope residues, as identified for the BCRTH01, INK09 and INK36
510 serum samples, are mapped on the surface of the RBD (PDB ID: 6M0J) and are color-coded
511 based on their epitope class. (B) Class 5/ RBD8 epitopes identified in this study are mapped
512 on the pre-fusion trimeric structure of the spike in its closed (PDB ID: 6VXX) and open (PDB
513 ID: 6VYB) conformations. (C) Matrix representing the conservation of identified epitope
514 residues across all major SARS-CoV-2 variants. Mutations of a specific residue in a particular
515 variant are represented in red square. Epitope classes are designated using coloured
516 diamonds.

517 **Figure 5. Mutation of epitope residues impacts the neutralizing activity of polyclonal**
518 **sera.** (A) Neutralization curves for pseudoviruses with WT (WA.1) or mutant spike proteins,
519 harbouring specific mutations at the epitope residues with serial dilutions of the BCRTH-01
520 serum. (B) Neutralization titers (IC_{50}) for WT and mutant pseudoviruses. (C-E) Neutralization
521 curves for WA.1, BA.1 and XBB.1.5 pseudoviruses with serial dilutions of BCRTH-01, INK-09
522 and INK-36 sera, respectively. (F) IC_{50} fold changes with respect to the WA.1.
523

524 **STAR Methods**

525

526 **Materials:**

527 **Cell line**

528 Human embryonic kidney (HEK) 293T cells (ATCC #CRL-3216) were maintained in
529 Dulbecco's modified Eagle's medium (DMEM) supplemented with 10% fetal bovine serum

530 (FBS) along with antibiotics like penicillin, streptomycin and anti mycotic agent (Gibco) at 37°C
531 and 5% CO_2.
532 **Plasmids:**
533 Plasmid pHAGE2-EF1aInt- ACE2-WT, expressing human ACE2 gene (BEI#NR-
534 52514) was used for overexpressing ACE2 in HEK 293T cells. Plasmid HDM-IDTSpike-fixK
535 (BEI#NR-52514) was used for expressing the codon-optimized spike protein from SARS-
536 CoV-2, Wuhan-Hu-1 strain (Genbank NC_045512). Plasmids pcDNA3.3-SARS2-B.1.617.1,
537 expressing spike protein of Kappa variant (addgene#172319), pcDNA3.3-SARS2-B.1.617.2
538 SARS-CoV-2, expressing spike protein of Delta variant (addgene#172320) [82] and SARS-
539 CoV-2 Omicron strain spike gene in Human codon_pcDNA3.1(+) expressing spike protein of
540 Omicron variant (B.1.1.529) (GenScript# MC_0101274) were utilized in the study [34]. XBB1.5
541 spike expression plasmid construct was a kind gift from Dr. Rajesh P. Ringe, Institute of
542 Microbial Technology, Council of Scientific and Industrial Research (CSIR), India.
543
544 **Antibodies:**
545 NB100-56578 is a polyclonal antibody raised in rabbits against SARS CoV-2 spike
546 protein and was obtained from Novus Biologicals (USA). Serum from the pre-COVID era
547 (Single donor human serum off the clot, ISERS2M-2019-33108-07) was obtained from
548 Innovative Research, Inc.
549
550 **Methodology:**
551
552 **Bioinformatics and Structural Analysis:**
553 Genome sequences of 47 different SARS-CoV-2 viruses that infect humans and 11
554 different sarbecovirus spike RBD sequences were obtained from the GISAID database.
555 Multiple sequence alignment was performed in Bioedit software using ClustalW multiple
556 alignment function. Further representation of the spike proteins' aligned RBD amino acid
557 sequences was performed using JALVIEW or the Multlin sequence alignment tool. Structural

558 alignment was performed in Pymol using specific PDB files of post-fusion spike protein
559 structures of SARS-CoV-2 viruses (PDB id: 6M0J).
560
561 **Construction of SARS-CoV-2 S mutant plasmid constructs:**
562 Plasmid HDM-IDTSpike-fixK expressing a codon-optimized spike protein from SARS-
563 CoV-2 was subjected to site-directed mutagenesis to generate R403D, G416D, T430D and
564 R466D, respectively, using the QuikChange II Site-directed mutagenesis kit (Agilent) according
565 to the manufacturer's instructions. Mutations generated in the SARS-CoV-2 S protein were
566 further verified using Sangers sequencing.
567
568 **Generation of SARS-CoV-2 S pseudotyped lentiviruses:**
569 Generation of SARS-CoV-2 lentivirus particles pseudotyped with either full-length WT,
570 different VoCs or mutation at SARS-CoV-2 spike protein (R403D, G416D, T430D and R466D)
571 were generated by transfecting HEK293T cells with the respective set of plasmids by using the
572 protocol as described previously by Crawford et al., 2020 [83]. Briefly, a lentiviral backbone
573 plasmid, pHAGE-CMV-Luc2-IRES-ZsGreen-W (BEI #NR-52516) bearing a CMV promoter to
574 express luciferase, was co-transfected with a set of other lentiviral plasmids like pHDM-
575 Hgpm2, expressing the HIV-1 gag and pol (BEI #NR-52517), pRC-CMV-rev1b, expressing the
576 HIV-1 rev (BEI #NR-52519), pHDM-tat1b, expressing the HIV-1 tat (BEI # NR- 52518), and
577 respective different WT or mutant spike protein-expressing plasmids. Post transfection, the
578 SARS CoV-2 pseudoviruses were collected by passing the supernatant through a 0.45 um
579 filter and used freshly.
580
581 **Pseudovirus-based Serum Neutralization Assay:**

582 Serum samples collected from the volunteers were inactivated at 65^0C for 30 minutes
583 prior to use. Serially diluted serum samples were incubated with either WT or different VoC/
584 mutant pseudoviruses at 37^0C for 1h. Serum-neutralized viral inoculum was then used to infect
585 hACE2-expressing HEK 293T cells at 37℃ for 1h in the CO_2 incubator in the presence of
586 polybrene till 18h. Successful neutralization of the pseudovirus results in a several fold
587 reduction in reporter virus activity, which were measured using a multimodal plate reader
588 (GloMax® Explorer Multimode Microplate Reader, Promega). Polyclonal SARS CoV-2
589 (NB100-56578) antibody served as a positive control, whereas sera from the pre-COVID era
590 were used as a negative control for the study.
591
592 **Charged scanning library construction and yeast surface display:**
593 Substitutions to Aspartate and Arginine are chosen for introduction in scanning
594 mutagenesis as analysis of existing DMS data suggests that these are the most disruptive for
595 binding. A charged scanning library of SARS CoV-2 spike RBD was generated using site-
596 directed mutagenesis. Exposed positions with accessibility >15% (total 125 residues) were
597 individually mutated to Aspartate or Arginine (for negatively charged residues), and each
598 mutant was fused by PCR to a unique 6 nucleotide barcode of known sequence to simplify
599 analysis and eliminate the need for long read sequencing. Upon mutagenesis by overlap PCR,
600 all the PCR products from each individual mutated position were pooled and transformed into
601 yeast via two fragment recombination by electroporation.
602
603 **Human sera screening**
604 Three human sera were selected for screening based on their high neutralization titres.
605 The sera were first titrated on yeast surface displaying WT-RBD and a saturating concentration
606 was chosen from the titration curve to be used for epitope mapping. The binding of these sera
607 with the aspartate library was analysed by flow cytometry, sorted into multiple gates and then
608 subjected to deep sequencing. Briefly, the pooled library of yeast cells expressing each of the
609 charged mutants was inoculated in 5 ml of SDCAA medium and grown overnight at 30°C, 250

610 rpm. The next day, a secondary inoculation from the overnight culture of the library was grown
611 at 30°C until an OD600 of 3–4, followed by induction in SGCAA medium at 20°C for 16 hr. A
612 total of 1× 10^7 cells of this library were washed twice with FACS buffer (1XPBS, pH 7.4 and
613 0.5% BSA) and then incubated at 4°C for 1 hr with a selected dilution of sera to probe for
614 binding and chicken anti-CMyc antibody (1:300 dilution) as a probe for the expression. The
615 cells were washed twice with FACS buffer and subsequently labelled with Alexa Fluor 633 goat
616 anti-human (1:1200 dilution) (catalogue no. A21091), plus Alexa Fluor 488 goat anti-chicken
617 (1:300 dilution), (catalogue no. A11039) for 20 min at room temperature in the dark. After
618 washing thrice with FACS buffer, cells were resuspended in 1 mL of FACS buffer, subjected to
619 flow cytometry, and sorted on an Aria-III cell sorter (BD Biosciences).
620
621 **Deep sequencing and analysis**
622 The sorted yeast cells from each gate were grown separately in liquid SDCAA medium
623 to saturation at 30°C for 24 hr, and the plasmids were extracted using EZ Yeast plasmid
624 miniprep kit (G Biosciences) according to the manufacturer's instructions and then subjected
625 to PCR. The PCR primers were designed to amplify the barcode region only (150 bp) and in a
626 way such that for both, the forward and reverse end reads, the first 3 bases are NNN followed
627 by 6 bases of unique sequence tag (MID) and the 21 bases of the primer sequence
628 complementary to the gene. Each forward MID sequence represents a particular serum, while
629 each reverse MID sequence represents a specific gate. The PCR for all the gates from three
630 sorted sera samples was carried out using Phusion polymerase for 15 cycles. Following
631 agarose gel electrophoresis and gel band purification, an equal amount (~100 ng) of PCR
632 product from each sample was pooled and then gel-band purified, followed by sequencing on
633 the NovaSeq platform. The fraction of each mutant (*Xi*) distributed across all the bins was
634 calculated as in (Equation 1) and then the reconstructed MFI for each mutant was calculated
635 by the summation of the product obtained from multiplying the fraction of a particular mutant
636 in a particular gate (*Xi*) with the MFI of that gate that was obtained from the FACS experiment
637 (*Fi*), (Equation 2).

Fraction of mutant in each gate $X_i = \frac{N_i}{\sum_1^n N_i}$ (Equation 1)

N*i*: Number of reads of a specific mutant in bin *i*.

Reconstructed MFI= $\sum_1^n X_i * N_i$ (Equation 2).

The ratio of MFI expression/MFI binding for all positions was represented by a heat map using GraphPad Prism software. The mutants with Ratio (Normalized MFI of expression: Normalized MFI of binding), one standard deviation higher than the mean MFI were considered as epitope residues.

Statistical analysis:

All experiments were performed in triplicates, and each data was repeated at least three times except for the epitope mapping experiments, which were performed in duplicates. Graphs are plotted using Graphpad Prism 10.1.2 and represented as mean standard deviations (n = 3). Results were compared by performing a two-tailed Student's t-test. Significance is defined as P < 0.05, and statistical significance is indicated with an asterisk (*). *P < 0.001 were considered statistically significant.

Supplementary information titles and legends

Supplementary information.
Document S1. Figures S1-S6 and Table S1-S2

References:

1. Ecdc.europa https://www.ecdc.europa.eu/en/covid-19/variants-concern.
2. Zabidi, N.Z., Liew, H.L., Farouk, I.A., Puniyamurti, A., Yip, A.J., Wijesinghe, V.N., Low, Z.Y., Tang, J.W., Chow, V.T.K., and Lal, S.K. (2023). Evolution of SARS-CoV-2 Variants: Implications on Immune Escape, Vaccination, Therapeutic and Diagnostic Strategies, https://doi.org/10.3390/v15040944 https://doi.org/10.3390/v15040944.
3. Our world in data https://ourworldindata.org/covid-vaccinations. covid 19 vaccinations india.
4. Doshi, R.H., Nsasiirwe, S., Dahlke, M., Atagbaza, A., Aluta, O.E., Tatsinkou, A.B., Dauda, E., Vilajeliu, A., Gurung, S., Tusiime, J., et al. (2024). COVID-19 Vaccination Coverage - World Health Organization African Region, 2021-2023. MMWR. Morbidity and mortality weekly report *73*, 307–311. https://doi.org/10.15585/mmwr.mm7314a3.
5. Ministry of health and family welfare, G. of I. Ministry of Health and Family Welfare

https://www.mohfw.gov.in Govt. Of India: COVID-19 data.

6. Sarkar, A., Chakrabarti, A.K., and Dutta, S. (2021). Covid-19 Infection in India: A Comparative Analysis of the Second Wave with the First Wave, https://doi.org/10.3390/pathogens10091222 https://doi.org/10.3390/pathogens10091222.

7. Tareq, A.M., Emran, T. Bin, Dhama, K., Dhawan, M., and Tallei, T.E. (2021). Impact of SARS-CoV-2 delta variant (B.1.617.2) in surging second wave of COVID-19 and efficacy of vaccines in tackling the ongoing pandemic. Human Vaccines & Immunotherapeutics *17*, 4126–4127. https://doi.org/10.1080/21645515.2021.1963601.

8. Chavda, V.P., Balar, P., Vaghela, D., Solanki, H.K., Vaishnav, A., Hala, V., and Vora, L. (2023). Omicron Variant of SARS-CoV-2: An Indian Perspective of Vaccination and Management, https://doi.org/10.3390/vaccines11010160 https://doi.org/10.3390/vaccines11010160.

9. Krishna, B., Gupta, A., Meena, K., Gaba, A., Krishna, S., Jyoti, R., Aeron, N., Prashanth, S., Samriti, and Ganapathy, U. (2022). Prevalence, severity, and risk factor of breakthrough infection after vaccination with either the Covaxin or the Covishield among healthcare workers: A nationwide cross-sectional study. Journal of anaesthesiology, clinical pharmacology *38*, S66–S78. https://doi.org/10.4103/joacp.joacp_436_21.

10. Kavitha, C., Gowrisankar, A., and Banerjee, S. (2021). The second and third waves in India: when will the pandemic be culminated? The European Physical Journal Plus *136*, 596. https://doi.org/10.1140/epjp/s13360-021-01586-7.

11. Letko, M., Marzi, A., and Munster, V. (2020). Functional assessment of cell entry and receptor usage for SARS-CoV-2 and other lineage B betacoronaviruses. Nature microbiology *5*, 562–569. https://doi.org/10.1038/s41564-020-0688-y.

12. Jackson, C.B., Farzan, M., Chen, B., and Choe, H. (2022). Mechanisms of SARS-CoV-2 entry into cells. Nature Reviews Molecular Cell Biology *23*, 3–20. https://doi.org/10.1038/s41580-021-00418-x.

13. Xiaojie, S., Yu, L., lei, Y., Guang, Y., and Min, Q. (2021). Neutralizing antibodies targeting SARS-CoV-2 spike protein. Stem Cell Research *50*, 102125. https://doi.org/https://doi.org/10.1016/j.scr.2020.102125.

14. Xia, S., Liu, M., Wang, C., Xu, W., Lan, Q., Feng, S., Qi, F., Bao, L., Du, L., Liu, S., et al. (2020). Inhibition of SARS-CoV-2 (previously 2019-nCoV) infection by a highly potent pan-coronavirus fusion inhibitor targeting its spike protein that harbors a high capacity to mediate membrane fusion. Cell Research *30*, 343–355. https://doi.org/10.1038/s41422-020-0305-x.

15. Du, L., He, Y., Zhou, Y., Liu, S., Zheng, B.-J., and Jiang, S. (2009). The spike protein of SARS-CoV — a target for vaccine and therapeutic development. Nature Reviews Microbiology *7*, 226–236. https://doi.org/10.1038/nrmicro2090.

16. Wrapp, D., Wang, N., Corbett, K.S., Goldsmith, J.A., Hsieh, C.L., Abiona, O., Graham, B.S., and McLellan, J.S. (2020). Cryo-EM structure of the 2019-nCoV spike in the prefusion conformation. Science *367*, 1260–1263. https://doi.org/10.1126/science.aax0902.

17. Piccoli, L., Park, Y.-J., Tortorici, M.A., Czudnochowski, N., Walls, A.C., Beltramello, M., Silacci-Fregni, C., Pinto, D., Rosen, L.E., Bowen, J.E., et al. (2020). Mapping Neutralizing and Immunodominant Sites on the SARS-CoV-2 Spike Receptor-Binding Domain by Structure-Guided High-Resolution Serology. Cell *183*, 1024-1042.e21. https://doi.org/10.1016/j.cell.2020.09.037.

18. Steffen, T.L., Stone, E.T., Hassert, M., Geerling, E., Grimberg, B.T., Espino, A.M., Pantoja, P., Climent, C., Hoft, D.F., George, S.L., et al. (2020). The receptor binding

723 domain of SARS-CoV-2 spike is the key target of neutralizing antibody in human
724 polyclonal sera. bioRxiv, 2020.08.21.261727.
725 https://doi.org/10.1101/2020.08.21.261727.

726 19. Greaney, A.J., Loes, A.N., Crawford, K.H.D., Starr, T.N., Malone, K.D., Chu, H.Y., and
727 Bloom, J.D. (2021). Comprehensive mapping of mutations in the SARS-CoV-2
728 receptor-binding domain that affect recognition by polyclonal human plasma
729 antibodies. Cell Host & Microbe *29*, 463-476.e6.
730 https://doi.org/https://doi.org/10.1016/j.chom.2021.02.003.

731 20. Chen, Y., Zhao, X., Zhou, H., Zhu, H., Jiang, S., and Wang, P. (2023). Broadly
732 neutralizing antibodies to SARS-CoV-2 and other human coronaviruses. Nature
733 Reviews Immunology *23*, 189–199. https://doi.org/10.1038/s41577-022-00784-3.

734 21. Barnes, C.O., Jette, C.A., Abernathy, M.E., Dam, K.-M.A., Esswein, S.R., Gristick,
735 H.B., Malyutin, A.G., Sharaf, N.G., Huey-Tubman, K.E., Lee, Y.E., et al. (2020).
736 SARS-CoV-2 neutralizing antibody structures inform therapeutic strategies. Nature
737 *588*, 682–687. https://doi.org/10.1038/s41586-020-2852-1.

738 22. Pinto, D., Park, Y.-J., Beltramello, M., Walls, A.C., Tortorici, M.A., Bianchi, S., Jaconi,
739 S., Culap, K., Zatta, F., De Marco, A., et al. (2020). Cross-neutralization of SARS-
740 CoV-2 by a human monoclonal SARS-CoV antibody. Nature *583*, 290–295.
741 https://doi.org/10.1038/s41586-020-2349-y.

742 23. Yuan, M., Wu, N.C., Zhu, X., Lee, C.-C.D., So, R.T.Y., Lv, H., Mok, C.K.P., and Wilson,
743 I.A. (2020). A highly conserved cryptic epitope in the receptor binding domains of
744 SARS-CoV-2 and SARS-CoV. Science *368*, 630–633.
745 https://doi.org/10.1126/science.abb7269.

746 24. Huang, Y., Yang, C., Xu, X. feng, Xu, W., and Liu, S. wen (2020). Structural and
747 functional properties of SARS-CoV-2 spike protein: potential antivirus drug
748 development for COVID-19. Acta Pharmacologica Sinica *41*, 1141–1149.
749 https://doi.org/10.1038/s41401-020-0485-4.

750 25. Liu, H., Wu, N.C., Yuan, M., Bangaru, S., Torres, J.L., Caniels, T.G., van Schooten, J.,
751 Zhu, X., Lee, C.-C.D., Brouwer, P.J.M., et al. (2020). Cross-Neutralization of a SARS-
752 CoV-2 Antibody to a Functionally Conserved Site Is Mediated by Avidity. Immunity *53*,
753 1272-1280.e5. https://doi.org/https://doi.org/10.1016/j.immuni.2020.10.023.

754 26. Jette, C.A., Cohen, A.A., Gnanapragasam, P.N.P., Muecksch, F., Lee, Y.E., Huey-
755 Tubman, K.E., Schmidt, F., Hatziioannou, T., Bieniasz, P.D., Nussenzweig, M.C., et al.
756 (2021). Broad cross-reactivity across sarbecoviruses exhibited by a subset of COVID-
757 19 donor-derived neutralizing antibodies. Cell Reports *36*, 109760.
758 https://doi.org/https://doi.org/10.1016/j.celrep.2021.109760.

759 27. Jensen, J.L., Sankhala, R.S., Dussupt, V., Bai, H., Hajduczki, A., Lal, K.G., Chang,
760 W.C., Martinez, E.J., Peterson, C.E., Golub, E.S., et al. (2023). Targeting the Spike
761 Receptor Binding Domain Class V Cryptic Epitope by an Antibody with Pan-
762 Sarbecovirus Activity. Journal of virology *97*, e0159622.
763 https://doi.org/10.1128/jvi.01596-22.

764 28. Rouet, R., Henry, J.Y., Johansen, M.D., Sobti, M., Balachandran, H., Langley, D.B.,
765 Walker, G.J., Lenthall, H., Jackson, J., Ubiparipovic, S., et al. (2023). Broadly
766 neutralizing SARS-CoV-2 antibodies through epitope-based selection from
767 convalescent patients. Nature Communications *14*, 687.
768 https://doi.org/10.1038/s41467-023-36295-5.

769 29. Chandra, S., Manjunath, K., Asok, A., and Varadarajan, R. (2023). Mutational scan
770 inferred binding energetics and structure in intrinsically disordered protein CcdA.
771 Protein science : a publication of the Protein Society *32*, e4580.
772 https://doi.org/10.1002/pro.4580.

773 30. Chandra, S., Chattopadhyay, G., and Varadarajan, R. (2021). Rapid Identification of
774 Secondary Structure and Binding Site Residues in an Intrinsically Disordered Protein

Segment. Frontiers in genetics *12*, 755292. https://doi.org/10.3389/fgene.2021.755292.

31. Bates, T.A., McBride, S.K., Leier, H.C., Guzman, G., Lyski, Z.L., Schoen, D., Winders, B., Lee, J.-Y., Lee, D.X., Messer, W.B., et al. (2022). Vaccination before or after SARS-CoV-2 infection leads to robust humoral response and antibodies that effectively neutralize variants. Science immunology *7*, eabn8014. https://doi.org/10.1126/sciimmunol.abn8014.

32. Walls, A.C., Sprouse, K.R., Bowen, J.E., Joshi, A., Franko, N., Navarro, M.J., Stewart, C., Cameroni, E., McCallum, M., Goecker, E.A., et al. (2022). SARS-CoV-2 breakthrough infections elicit potent, broad, and durable neutralizing antibody responses. Cell *185*, 872-880.e3. https://doi.org/https://doi.org/10.1016/j.cell.2022.01.011.

33. Swami, A., Mohanty, A., Jamwal, A., Turbadkar, D., Baveja, S., Shastri, J., and Chitalia, V. (2023). A comparative analysis of the second and third wave of the Covid-19 pandemic: an experience from a tertiary care hospital in Western India. Journal of medical microbiology *72*. https://doi.org/10.1099/jmm.0.001685.

34. Jana, I. Das, Bhattacharya, P., Mayilsamy, K., Banerjee, S., Bhattacharje, G., Das, S., Aditya, S., Ghosh, A., McGill, A.R., Srikrishnan, S., et al. (2022). Targeting an evolutionarily conserved “e-L-L” motif in spike protein to identify a small molecule fusion inhibitor against SARS-CoV-2. PNAS Nexus *1*, 1–14. https://doi.org/10.1093/pnasnexus/pgac198.

35. Wenlin, R., Xiaohui, J., Mingli, G., Jun, L., Yanying, Y., Quanxin, L., J., K.D., K., O.A., Yu, Z., Jin, Z., et al. (2022). Characterization of SARS-CoV-2 Variants B.1.617.1 (Kappa), B.1.617.2 (Delta), and B.1.618 by Cell Entry and Immune Evasion. mBio *13*, e00099-22. https://doi.org/10.1128/mbio.00099-22.

36. Servellita, V., Syed, A.M., Morris, M.K., Brazer, N., Saldhi, P., Garcia-Knight, M., Sreekumar, B., Khalid, M.M., Ciling, A., Chen, P.-Y., et al. (2022). Neutralizing immunity in vaccine breakthrough infections from the SARS-CoV-2 Omicron and Delta variants. Cell *185*, 1539-1548.e5. https://doi.org/https://doi.org/10.1016/j.cell.2022.03.019.

37. Ai, J., Zhang, H., Zhang, Y., Lin, K., Zhang, Y., Wu, J., Wan, Y., Huang, Y., Song, J., Fu, Z., et al. (2022). Omicron variant showed lower neutralizing sensitivity than other SARS-CoV-2 variants to immune sera elicited by vaccines after boost. Emerging Microbes & Infections *11*, 337–343. https://doi.org/10.1080/22221751.2021.2022440.

38. Greaney, A.J., Starr, T.N., Barnes, C.O., Weisblum, Y., Schmidt, F., Caskey, M., Gaebler, C., Cho, A., Agudelo, M., Finkin, S., et al. (2021). Mapping mutations to the SARS-CoV-2 RBD that escape binding by different classes of antibodies. Nature Communications *12*, 4196. https://doi.org/10.1038/s41467-021-24435-8.

39. Wang, Q., Iketani, S., Li, Z., Liu, L., Guo, Y., Huang, Y., Bowen, A.D., Liu, M., Wang, M., Yu, J., et al. (2023). Alarming antibody evasion properties of rising SARS-CoV-2 BQ and XBB subvariants. Cell *186*, 279-286.e8. https://doi.org/10.1016/j.cell.2022.12.018.

40. Kugathasan, R., Sukhova, K., Moshe, M., Kellam, P., and Barclay, W. (2023). Deep mutagenesis scanning using whole trimeric SARS-CoV-2 spike highlights the importance of NTD-RBD interactions in determining spike phenotype. PLoS pathogens *19*, e1011545. https://doi.org/10.1371/journal.ppat.1011545.

41. Greaney, A.J., Eguia, R.T., Starr, T.N., Khan, K., Franko, N., Logue, J.K., Lord, S.M., Speake, C., Chu, H.Y., Sigal, A., et al. (2022). The SARS-CoV-2 Delta variant induces an antibody response largely focused on class 1 and 2 antibody epitopes. PLOS Pathogens *18*, e1010592.

42. Tanaka, S., Olson, C.A., Barnes, C.O., Higashide, W., Gonzalez, M., Taft, J., Richardson, A., Martin-Fernandez, M., Bogunovic, D., Gnanapragasam, P.N.P., et al.

(2022). Rapid identification of neutralizing antibodies against SARS-CoV-2 variants by mRNA display. Cell Reports *38*, 110348. https://doi.org/https://doi.org/10.1016/j.celrep.2022.110348.

43. Rao, X., Zhao, R., Tong, Z., Guo, S., Peng, W., Liu, K., Li, S., Wu, L., Tong, J., Chai, Y., et al. (2023). Defining a de novo non-RBM antibody as RBD-8 and its synergistic rescue of immune-evaded antibodies to neutralize Omicron SARS-CoV-2. Proceedings of the National Academy of Sciences *120*, e2314193120. https://doi.org/10.1073/pnas.2314193120.

44. Sankhala, R.S., Dussupt, V., Chen, W.-H., Bai, H., Martinez, E.J., Jensen, J.L., Rees, P.A., Hajduczki, A., Chang, W.C., Choe, M., et al. (2024). Antibody targeting of conserved sites of vulnerability on the SARS-CoV-2 spike receptor-binding domain. Structure (London, England : 1993) *32*, 131-147.e7. https://doi.org/10.1016/j.str.2023.11.015.

45. Starr, T.N., Czudnochowski, N., Liu, Z., Zatta, F., Park, Y.-J., Addetia, A., Pinto, D., Beltramello, M., Hernandez, P., Greaney, A.J., et al. (2021). SARS-CoV-2 RBD antibodies that maximize breadth and resistance to escape. Nature *597*, 97–102. https://doi.org/10.1038/s41586-021-03807-6.

46. Hotez, P. (2023). XBB.1.5 emerges in the Americas: what it means to the region. Lancet regional health. Americas *18*, 100433. https://doi.org/10.1016/j.lana.2023.100433.

47. Callaway, E. (2023). Coronavirus variant XBB.1.5 rises in the United States - is it a global threat?, https://doi.org/10.1038/d41586-023-00014-3 https://doi.org/10.1038/d41586-023-00014-3.

48. Ao, D., He, X., Hong, W., and Wei, X. (2023). The rapid rise of SARS-CoV-2 Omicron subvariants with immune evasion properties: XBB.1.5 and BQ.1.1 subvariants. MedComm *4*, e239. https://doi.org/10.1002/mco2.239.

49. Parums, D. V (2023). Editorial: The XBB.1.5 ('Kraken') Subvariant of Omicron SARS-CoV-2 and its Rapid Global Spread., https://doi.org/10.12659/MSM.939580 https://doi.org/10.12659/MSM.939580.

50. Machado, R.R.G., Candido, É.D., Aguiar, A.S., Chalup, V.N., Sanches, P.R., Dorlass, E.G., Amgarten, D.E., Pinho, J.R.R., Durigon, E.L., and Oliveira, D.B.L. (2024). Immune Evasion of SARS-CoV-2 Omicron Subvariants XBB.1.5, XBB.1.16 and EG.5.1 in a Cohort of Older Adults after ChAdOx1-S Vaccination and BA.4/5 Bivalent Booster. Vaccines *12*. https://doi.org/10.3390/vaccines12020144.

51. Chen, J.-J., Li, L.-B., Peng, H.-H., Tian, S., Ji, B., Shi, C., Qian, C., Jiang, W.-G., Liu, M.-C., Li, T.-T., et al. (2023). Neutralization against XBB.1 and XBB.1.5 after omicron subvariants breakthrough infection or reinfection. The Lancet regional health. Western Pacific *33*, 100759. https://doi.org/10.1016/j.lanwpc.2023.100759.

52. Cao, Y., Jian, F., Wang, J., Yu, Y., Song, W., Yisimayi, A., Wang, J., An, R., Chen, X., Zhang, N., et al. (2023). Imprinted SARS-CoV-2 humoral immunity induces convergent Omicron RBD evolution. Nature *614*, 521–529. https://doi.org/10.1038/s41586-022-05644-7.

53. Jian, F., Feng, L., Yang, S., Yu, Y., Wang, L., Song, W., Yisimayi, A., Chen, X., Xu, Y., Wang, P., et al. (2023). Convergent evolution of SARS-CoV-2 XBB lineages on receptor-binding domain 455-456 synergistically enhances antibody evasion and ACE2 binding. PLoS pathogens *19*, e1011868. https://doi.org/10.1371/journal.ppat.1011868.

54. Kitchin, D., Richardson, S.I., van der Mescht, M.A., Motlou, T., Mzindle, N., Moyo-Gwete, T., Makhado, Z., Ayres, F., Manamela, N.P., Spencer, H., et al. (2022). Ad26.COV2.S breakthrough infections induce high titers of neutralizing antibodies against Omicron and other SARS-CoV-2 variants of concern. Cell Reports Medicine *3*, 100535. https://doi.org/https://doi.org/10.1016/j.xcrm.2022.100535.

55. Nutalai, R., Zhou, D., Tuekprakhon, A., Ginn, H.M., Supasa, P., Liu, C., Huo, J., Mentzer, A.J., Duyvesteyn, H.M.E., Dijokaite-Guraliuc, A., et al. (2022). Potent cross-reactive antibodies following Omicron breakthrough in vaccinees. Cell *185*, 2116-2131.e18. https://doi.org/https://doi.org/10.1016/j.cell.2022.05.014.

56. Carr, E.J., Wu, M.Y., Gahir, J., Harvey, R., Townsley, H., Bailey, C., Fowler, A.S., Dowgier, G., Hobbs, A., Herman, L., et al. (2023). Neutralising immunity to omicron sublineages BQ.1.1, XBB, and XBB.1.5 in healthy adults is boosted by bivalent BA.1-containing mRNA vaccination and previous Omicron infection., https://doi.org/10.1016/S1473-3099(23)00289-X https://doi.org/10.1016/S1473-3099(23)00289-X.

57. Nham, E., Kim, J., Lee, J., Park, H., Kim, J., Lee, S., Choi, J., Kim, K.T., Yoon, J.G., Hwang, S.Y., et al. (2023). Low Neutralizing Activities to the Omicron Subvariants BN.1 and XBB.1.5 of Sera From the Individuals Vaccinated With a BA.4/5-Containing Bivalent mRNA Vaccine. Immune network *23*, e43. https://doi.org/10.4110/in.2023.23.e43.

58. Qian Wang , Yicheng Guo , Anthony Bowen , Ian A Mellis , Riccardo Valdez , Carmen Gherasim , Abree Gordon , Lihong Liu, D.D.H. (2024). XBB.1.5 monovalent mRNA vaccine booster elicits robust neutralizing antibodies against XBB subvariants and JN.1. Cell host & microbe *32*, 315-321.e3. https://doi.org/10.1016/j.chom.2024.01.014.

59. Greaney, A.J., Starr, T.N., Gilchuk, P., Zost, S.J., Binshtein, E., Loes, A.N., Hilton, S.K., Huddleston, J., Eguia, R., Crawford, K.H.D., et al. (2021). Complete Mapping of Mutations to the SARS-CoV-2 Spike Receptor-Binding Domain that Escape Antibody Recognition. Cell host & microbe *29*, 44-57.e9. https://doi.org/10.1016/j.chom.2020.11.007.

60. Raksha, D., Rohini, D., and Raghavan, V. (2020). Probing the Structure of the HIV-1 Envelope Trimer Using Aspartate Scanning Mutagenesis. Journal of Virology *94*, 10.1128/jvi.01426-20. https://doi.org/10.1128/jvi.01426-20.

61. Greaney, A.J., Loes, A.N., Gentles, L.E., Crawford, K.H.D., Starr, T.N., Malone, K.D., Chu, H.Y., and Bloom, J.D. (2021). Antibodies elicited by mRNA-1273 vaccination bind more broadly to the receptor binding domain than do those from SARS-CoV-2 infection. Science translational medicine *13*. https://doi.org/10.1126/scitranslmed.abi9915.

62. Bajaj, K., Chakrabarti, P., and Varadarajan, R. (2005). Mutagenesis-based definitions and probes of residue burial in proteins. Proceedings of the National Academy of Sciences *102*, 16221–16226. https://doi.org/10.1073/pnas.0505089102.

63. Cao, Y., Yisimayi, A., Jian, F., Song, W., Xiao, T., Wang, L., Du, S., Wang, J., Li, Q., Chen, X., et al. (2022). BA.2.12.1, BA.4 and BA.5 escape antibodies elicited by Omicron infection. Nature *608*, 593–602. https://doi.org/10.1038/s41586-022-04980-y.

64. Rappazzo, C.G., Tse, L. V, Kaku, C.I., Wrapp, D., Sakharkar, M., Huang, D., Deveau, L.M., Yockachonis, T.J., Herbert, A.S., Battles, M.B., et al. (2021). Broad and potent activity against SARS-like viruses by an engineered human monoclonal antibody. Science (New York, N.Y.) *371*, 823–829. https://doi.org/10.1126/science.abf4830.

65. Cao, Y., Wang, J., Jian, F., Xiao, T., Song, W., Yisimayi, A., Huang, W., Li, Q., Wang, P., An, R., et al. (2022). Omicron escapes the majority of existing SARS-CoV-2 neutralizing antibodies. Nature *602*, 657–663. https://doi.org/10.1038/s41586-021-04385-3.

66. Joseph, J., Darpe, S., Kulkarni, G., and Raj, V.S. (2023). SARS-CoV-2 neutralizing antibody epitopes are overlapping and highly mutated which raises the chances of escape variants and requires development of broadly reactive vaccines. Proteins *91*, 1021–1031. https://doi.org/10.1002/prot.26488.

67. Miller, J., Hachmann, N.P., Collier, A.-R.Y., Lasrado, N., Mazurek, C.R., Patio, R.C.,

Powers, O., Surve, N., Theiler, J., Korber, B., et al. (2023). Substantial Neutralization Escape by SARS-CoV-2 Omicron Variants BQ.1.1 and XBB.1., https://doi.org/10.1056/NEJMc2214314 https://doi.org/10.1056/NEJMc2214314.

68. Dejnirattisai, W., Zhou, D., Ginn, H.M., Duyvesteyn, H.M.E., Supasa, P., Case, J.B., Zhao, Y., Walter, T.S., Mentzer, A.J., Liu, C., et al. (2021). The antigenic anatomy of SARS-CoV-2 receptor binding domain. Cell *184*, 2183-2200.e22. https://doi.org/https://doi.org/10.1016/j.cell.2021.02.032.

69. Huang, K.-Y.A., Tan, T.K., Chen, T.-H., Huang, C.-G., Harvey, R., Hussain, S., Chen, C.-P., Harding, A., Gilbert-Jaramillo, J., Liu, X., et al. (2021). Correction: Breadth and function of antibody response to acute SARS-CoV-2 infection in humans. PLOS Pathogens *17*, e1010148.

70. Tortorici, M.A., Beltramello, M., Lempp, F.A., Pinto, D., Dang, H. V, Rosen, L.E., McCallum, M., Bowen, J., Minola, A., Jaconi, S., et al. (2020). Ultrapotent human antibodies protect against SARS-CoV-2 challenge via multiple mechanisms. Science *370*, 950–957. https://doi.org/10.1126/science.abe3354.

71. Tortorici, M.A., Czudnochowski, N., Starr, T.N., Marzi, R., Walls, A.C., Zatta, F., Bowen, J.E., Jaconi, S., Di Iulio, J., Wang, Z., et al. (2021). Broad sarbecovirus neutralization by a human monoclonal antibody. Nature *597*, 103–108. https://doi.org/10.1038/s41586-021-03817-4.

72. Wang, R., Chen, J., Gao, K., and Wei, G.-W. (2021). Vaccine-escape and fast-growing mutations in the United Kingdom, the United States, Singapore, Spain, India, and other COVID-19-devastated countries. Genomics *113*, 2158–2170. https://doi.org/https://doi.org/10.1016/j.ygeno.2021.05.006.

73. Veronika, T., Hemantha, K., Lydia, L., Victoria, B., Elena, R., Dagmara, K., Yulia, S., Debarati, C., Iryna, M., Kai, D., et al. (2021). Acquisition of the L452R Mutation in the ACE2-Binding Interface of Spike Protein Triggers Recent Massive Expansion of SARS-CoV-2 Variants. Journal of Clinical Microbiology *59*, 10.1128/jcm.00921-21. https://doi.org/10.1128/jcm.00921-21.

74. Kurhade, C., Zou, J., Xia, H., Liu, M., Chang, H.C., Ren, P., Xie, X., and Shi, P. (2023). Low neutralization of SARS-CoV-2 Omicron BA.2.75.2, BQ.1.1 and XBB.1 by parental mRNA vaccine or a BA.5 bivalent booster. Nature Medicine *29*, 344–347. https://doi.org/10.1038/s41591-022-02162-x.

75. Parums, D. V (2023). Editorial: A Rapid Global Increase in COVID-19 is Due to the Emergence of the EG.5 (Eris) Subvariant of Omicron SARS-CoV-2., https://doi.org/10.12659/MSM.942244 https://doi.org/10.12659/MSM.942244.

76. Vellas, C., Trémeaux, P., Del Bello, A., Latour, J., Jeanne, N., Ranger, N., Danet, C., Martin-Blondel, G., Delobel, P., Kamar, N., et al. (2022). Resistance mutations in SARS-CoV-2 omicron variant in patients treated with sotrovimab. Clinical Microbiology and Infection *28*, 1297–1299. https://doi.org/https://doi.org/10.1016/j.cmi.2022.05.002.

77. Xiong, H., Sun, H., Wang, S., Yuan, L., Liu, L., Zhu, Y., Zhang, J., Huang, Y., Qi, R., Jiang, Y., et al. (2022). The neutralizing breadth of antibodies targeting diverse conserved epitopes between SARS-CoV and SARS-CoV-2. Proceedings of the National Academy of Sciences *119*, e2204256119. https://doi.org/10.1073/pnas.2204256119.

78. Li, T., Xue, W., Zheng, Q., Song, S., Yang, C., Xiong, H., Zhang, S., Hong, M., Zhang, Y., Yu, H., et al. (2021). Cross-neutralizing antibodies bind a SARS-CoV-2 cryptic site and resist circulating variants. Nature Communications *12*, 5652. https://doi.org/10.1038/s41467-021-25997-3.

79. Starr, T.N., Greaney, A.J., Dingens, A.S., and Bloom, J.D. (2021). Complete map of SARS-CoV-2 RBD mutations that escape the monoclonal antibody LY-CoV555 and its cocktail with LY-CoV016. Cell Reports Medicine *2*, 100255. https://doi.org/https://doi.org/10.1016/j.xcrm.2021.100255.

80. Hastie, K.M., Li, H., Bedinger, D., Schendel, S.L., Dennison, S.M., Li, K., Rayaprolu, V., Yu, X., Mann, C., Zandonatti, M., et al. (2021). Defining variant-resistant epitopes targeted by SARS-CoV-2 antibodies: A global consortium study. Science *374*, 472–478. https://doi.org/10.1126/science.abh2315.

81. Martinez, D.R., Schäfer, A., Gobeil, S., Li, D., De la Cruz, G., Parks, R., Lu, X., Barr, M., Stalls, V., Janowska, K., et al. (2024). A broadly cross-reactive antibody neutralizes and protects against sarbecovirus challenge in mice. Science Translational Medicine *14*, eabj7125. https://doi.org/10.1126/scitranslmed.abj7125.

82. Cho, H., Gonzales-Wartz, K.K., Huang, D., Yuan, M., Peterson, M., Liang, J., Beutler, N., Torres, J.L., Cong, Y., Postnikova, E., et al. (2024). Bispecific antibodies targeting distinct regions of the spike protein potently neutralize SARS-CoV-2 variants of concern. Science Translational Medicine *13*, eabj5413. https://doi.org/10.1126/scitranslmed.abj5413.

83. Crawford, K.H.D., Eguia, R., Dingens, A.S., Loes, A.N., Malone, K.D., Wolf, C.R., Chu, H.Y., Tortorici, M.A., Veesler, D., Murphy, M., et al. (2020). Protocol and reagents for pseudotyping lentiviral particles with SARS-CoV-2 spike protein for neutralization assays. Viruses *12*. https://doi.org/10.3390/v12050513.

84. Li, T., Cai, H., Zhao, Y., Li, Y., Lai, Y., Yao, H., Liu, L.D., Sun, Z., van Vlissingen, M.F., Kuiken, T., et al. (2021). Uncovering a conserved vulnerability site in SARS-CoV-2 by a human antibody. EMBO molecular medicine *13*, e14544. https://doi.org/10.15252/emmm.202114544.

85. Bullen, G., Galson, J.D., Hall, G., Villar, P., Moreels, L., Ledsgaard, L., Mattiuzzo, G., Bentley, E.M., Masters, E.W., Tang, D., et al. (2021). Cross-Reactive SARS-CoV-2 Neutralizing Antibodies From Deep Mining of Early Patient Responses. Frontiers in immunology *12*, 678570. https://doi.org/10.3389/fimmu.2021.678570.

86. Wu, N.C., Yuan, M., Bangaru, S., Huang, D., Zhu, X., Lee, C.-C.D., Turner, H.L., Peng, L., Yang, L., Burton, D.R., et al. (2020). A natural mutation between SARS-CoV-2 and SARS-CoV determines neutralization by a cross-reactive antibody. PLOS Pathogens *16*, e1009089.

87. Barnes, C.O., West, A.P.J., Huey-Tubman, K.E., Hoffmann, M.A.G., Sharaf, N.G., Hoffman, P.R., Koranda, N., Gristick, H.B., Gaebler, C., Muecksch, F., et al. (2020). Structures of Human Antibodies Bound to SARS-CoV-2 Spike Reveal Common Epitopes and Recurrent Features of Antibodies. Cell *182*, 828-842.e16. https://doi.org/10.1016/j.cell.2020.06.025.

1026

1027

1028

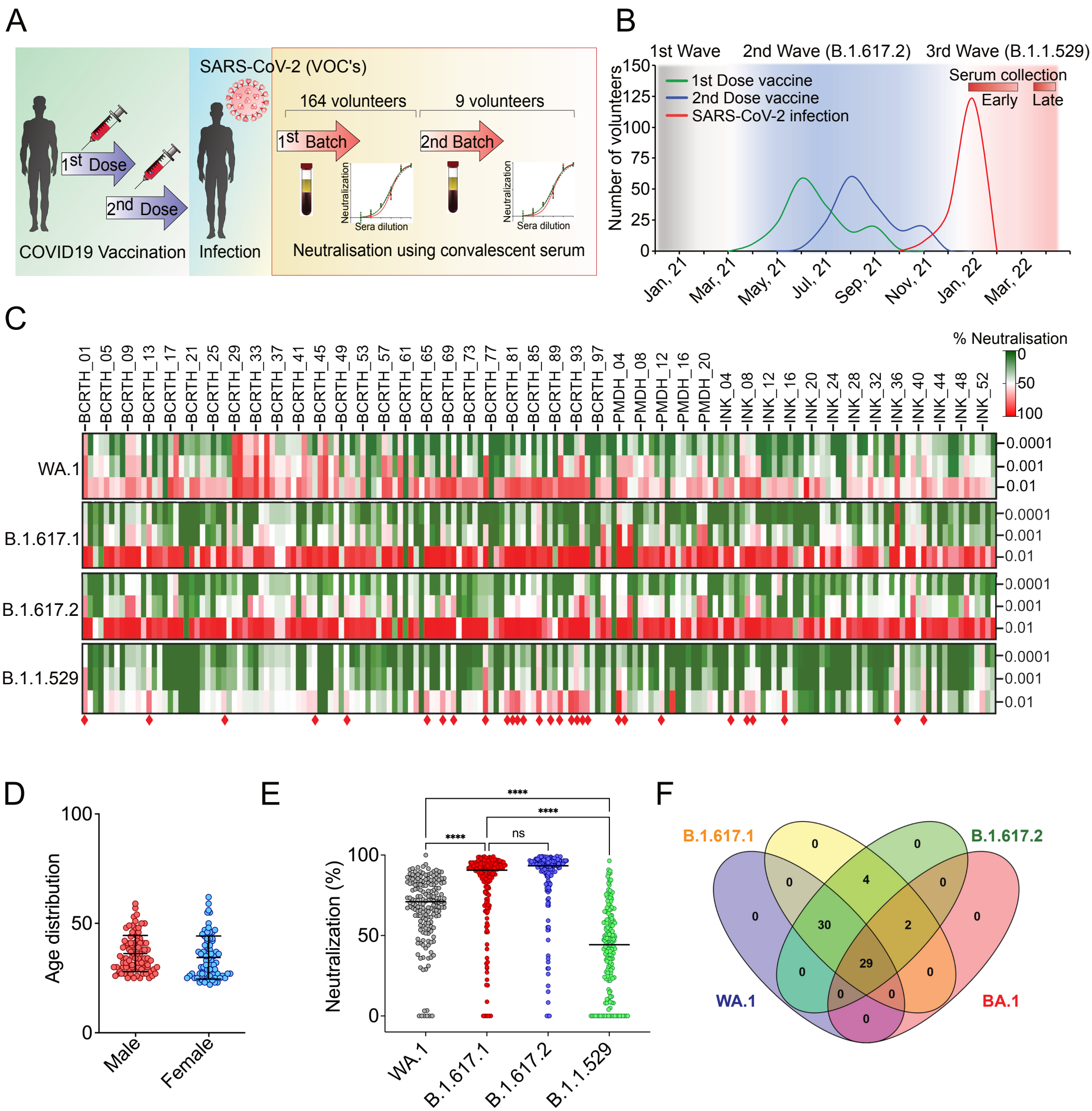
A
1st Dose
2nd Dose
COVID19 Vaccination
SARS-CoV-2 (VOC's)
Infection
164 volunteers
9 volunteers
1st Batch
2nd Batch
Neutralization
Sera dilution
Neutralisation using convalescent serum
B
1st Wave
2nd Wave (B.1.617.2)
3rd Wave (B.1.1.529)
1st Dose vaccine
2nd Dose vaccine
SARS-CoV-2 infection
Serum collection
Early
Late
Number of volunteers
Jan, 21
Mar, 21
May, 21
Jul, 21
Sep, 21
Nov, 21
Jan, 22
Mar, 22
C
% Neutralisation
WA.1
B.1.617.1
B.1.617.2
B.1.1.529
0.0001
0.001
0.01
D
Age distribution
Male
Female
E
Neutralization (%)
****
ns
WA.1
B.1.617.1
B.1.617.2
B.1.1.529
F
B.1.617.1
B.1.617.2
WA.1
BA.1

Figure 1

A

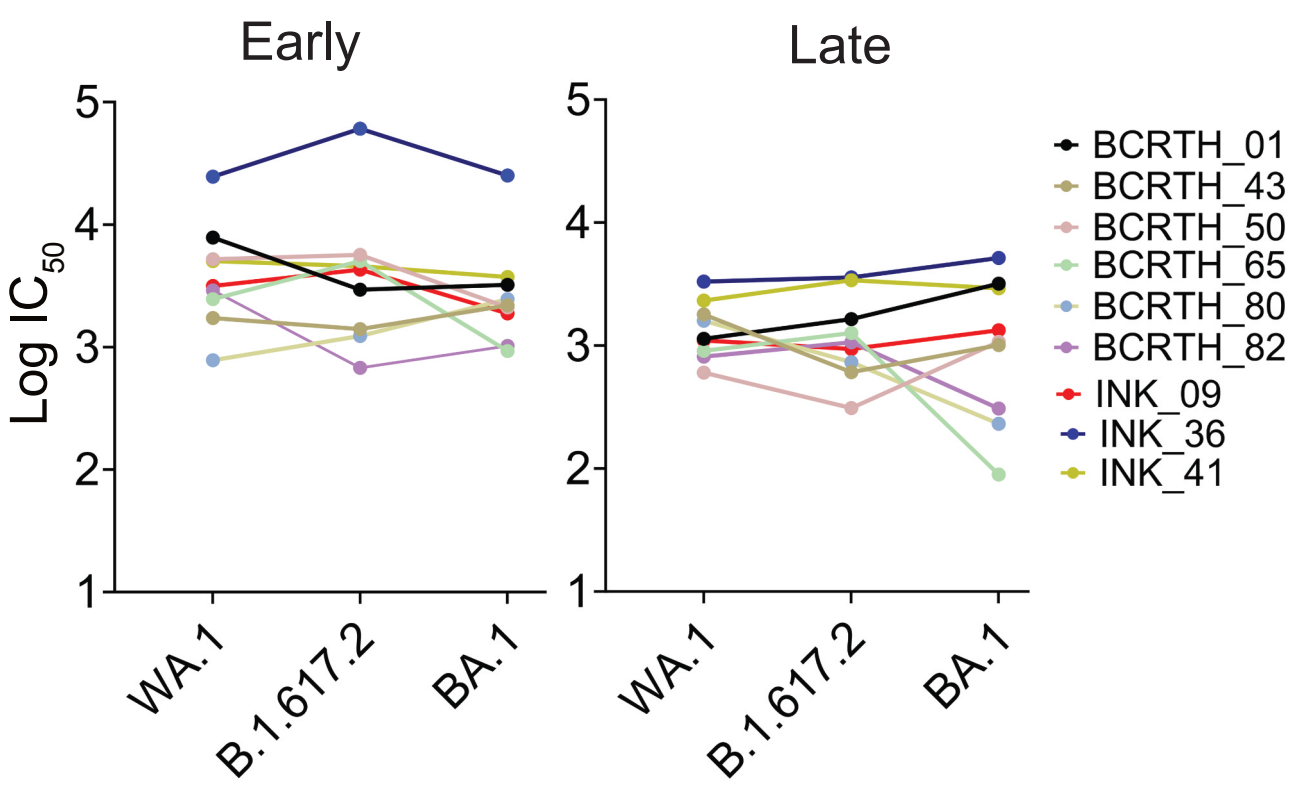

B

Early

	WA.1	B.1.617.2	BA.1
BCRTH01	1	0.37	0.41
BCRTH43	1	0.81	1.27
BCRTH50	1	1.08	0.4
BCRTH65	1	2.04	0.38
BCRTH80	1	1.58	3.16
BCRTH82	1	0.23	0.35
INK09	1	1.36	0.6
INK36	1	2.47	1.02
INK41	1	0.91	0.74

0.23
3.16

Late

	WA.1	B.1.617.2	BA.1
BCRTH01	1	1.45	2.81
BCRTH43	1	0.34	0.56
BCRTH50	1	0.51	1.78
BCRTH65	1	1.40	0.10
BCRTH80	1	0.46	0.15
BCRTH82	1	1.31	0.38
INK09	1	0.85	1.21
INK36	1	1.08	1.56
INK_41	1	1.47	1.26

0.10
2.81

C

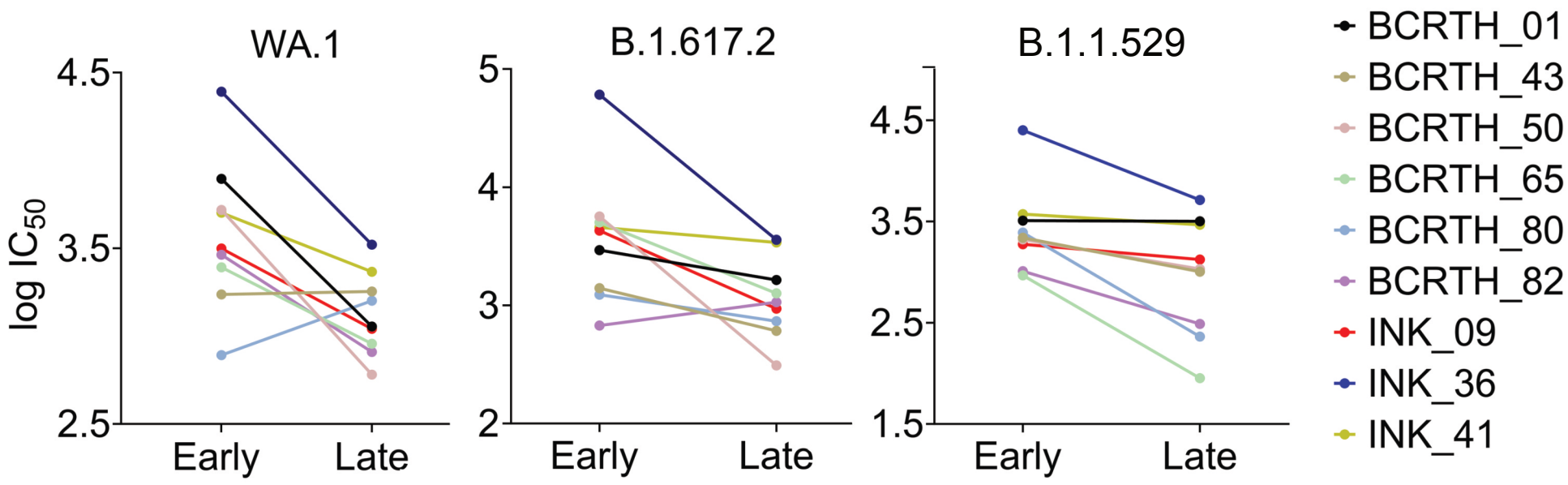

D

	BCRTH01	BCRTH43	BCRTH50	BCRTH65	BCRTH80	BCRTH82	INK09	INK36	INK_41
WA.1	0.14	1.04	0.12	0.37	2.04	0.28	0.35	0.13	0.46
B.1.617.2	0.56	0.43	0.05	0.25	0.6	1.57	0.22	0.06	0.74
BA.1	0.99	0.46	0.51	0.1	0.09	0.3	0.71	0.21	0.78

Fold change
Increase
Decrease

Figure 2

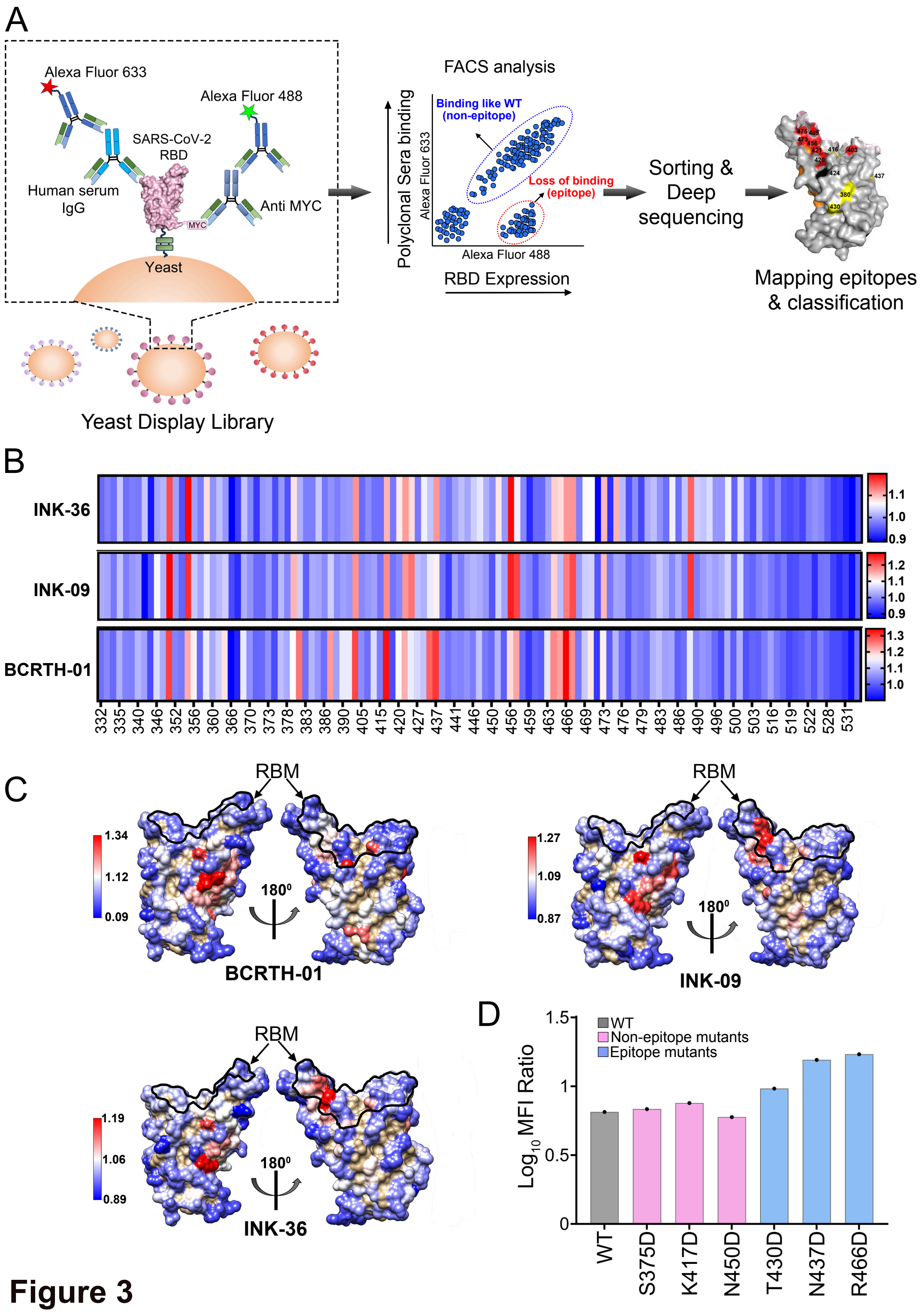
A
Alexa Fluor 633
Alexa Fluor 488
SARS-CoV-2 RBD
Human serum IgG
Anti MYC
MYC
Yeast
Yeast Display Library
FACS analysis
Polyclonal Sera binding
Alexa Fluor 633
Binding like WT (non-epitope)
Loss of binding (epitope)
Alexa Fluor 488
RBD Expression
Sorting & Deep sequencing
Mapping epitopes & classification
B
INK-36
INK-09
BCRTH-01
332 335 340 346 352 356 360 366 370 373 378 383 386 390 405 415 420 427 437 441 446 450 456 459 463 466 469 473 476 479 483 486 490 496 500 503 516 519 522 528 531
C
RBM
180⁰
BCRTH-01
INK-09
INK-36
D
WT
Non-epitope mutants
Epitope mutants
Log10 MFI Ratio
WT
S375D
K417D
N450D
T430D
N437D
R466D

Figure 3

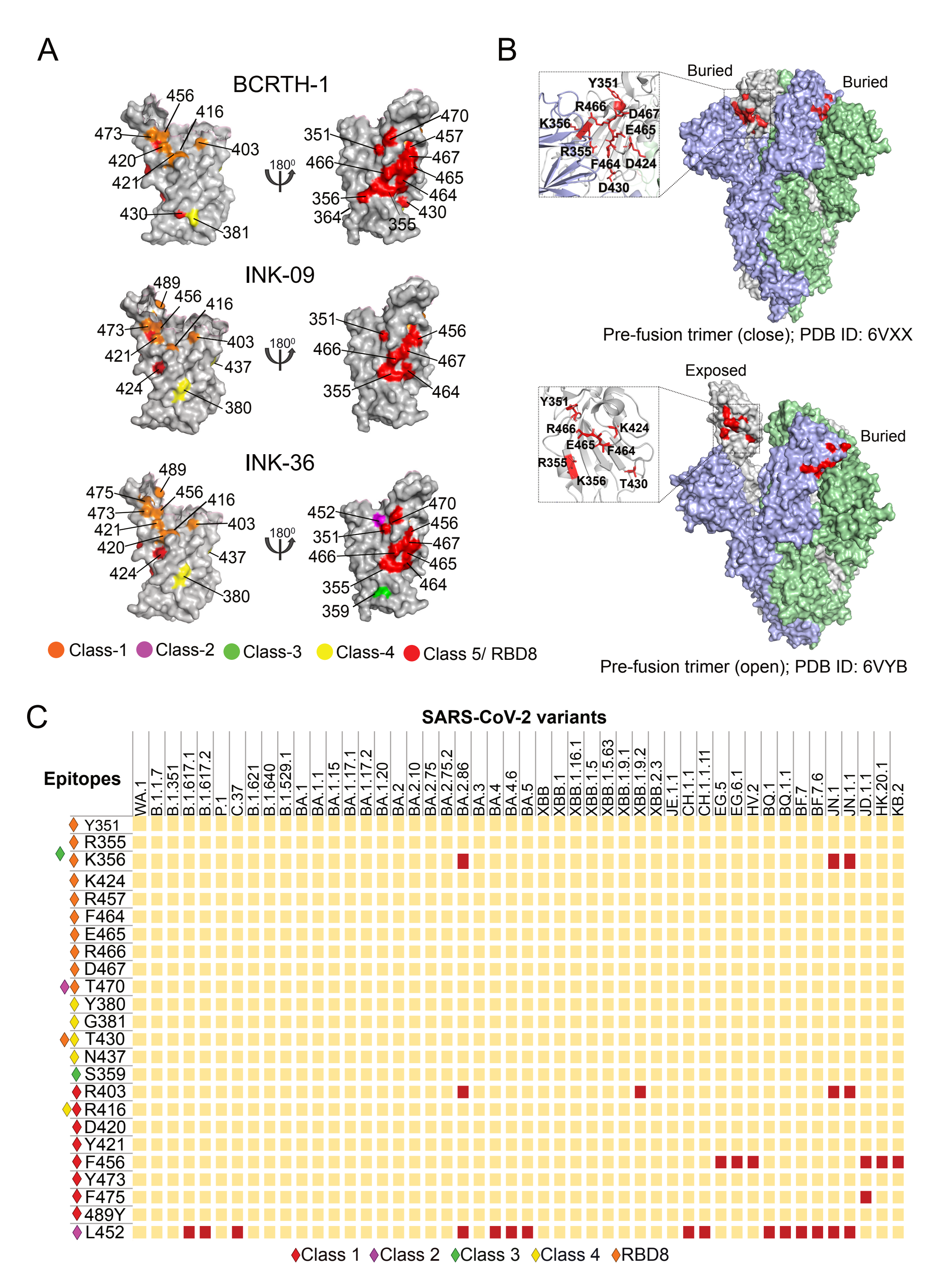
A
BCRTH-1
456
416
473
403
420
421
430
381
180⁰
351
470
457
466
467
465
356
464
364
430
355
INK-09
489
456
416
473
403
421
437
424
380
180⁰
351
456
466
467
355
464
INK-36
489
475
456
416
473
403
421
420
437
424
380
180⁰
452
470
351
456
466
467
465
355
464
359
Class-1
Class-2
Class-3
Class-4
Class 5/ RBD8
B
Buried
Buried
Y351
R466
D467
K356
E465
R355
F464
D424
D430
Pre-fusion trimer (close); PDB ID: 6VXX
Exposed
Buried
Y351
R466
K424
E465
F464
R355
K356
T430
Pre-fusion trimer (open); PDB ID: 6VYB
C
SARS-CoV-2 variants
Epitopes
WA.1
B.1.1.7
B.1.351
B.1.617.1
B.1.617.2
P.1
C.37
B.1.621
B.1.640
B.1.529.1
BA.1
BA.1.1
BA.1.15
BA.1.17.1
BA.1.17.2
BA.1.20
BA.2
BA.2.10
BA.2.75
BA.2.75.2
BA.2.86
BA.3
BA.4
BA.4.6
BA.5
XBB
XBB.1
XBB.1.16.1
XBB.1.5
XBB.1.5.63
XBB.1.9.1
XBB.1.9.2
XBB.2.3
JE.1.1
CH.1.1
CH.1.1.11
EG.5
EG.6.1
HV.2
BQ.1
BQ.1.1
BF.7
BF.7.6
JN.1
JN.1.1
JD.1.1
HK.20.1
KB.2
Y351
R355
K356
K424
R457
F464
E465
R466
D467
T470
Y380
G381
T430
N437
S359
R403
R416
D420
Y421
F456
Y473
F475
489Y
L452
Class 1
Class 2
Class 3
Class 4
RBD8

Figure 4

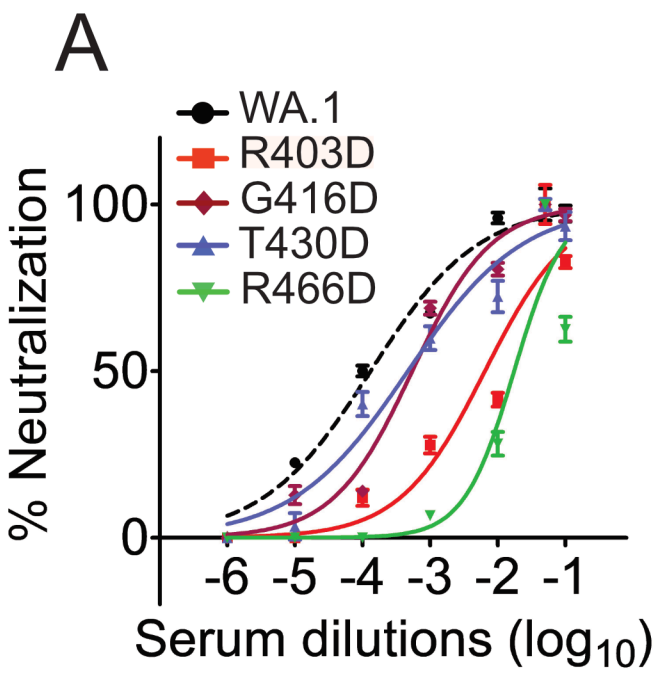

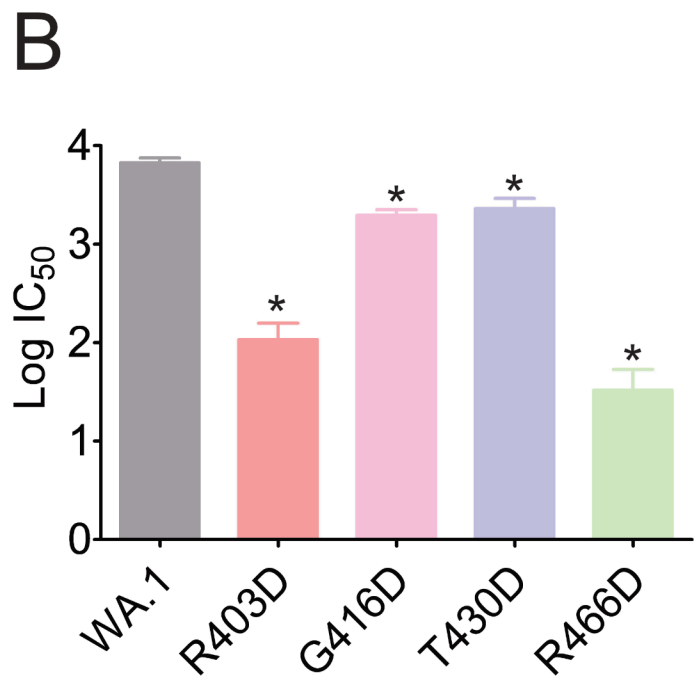

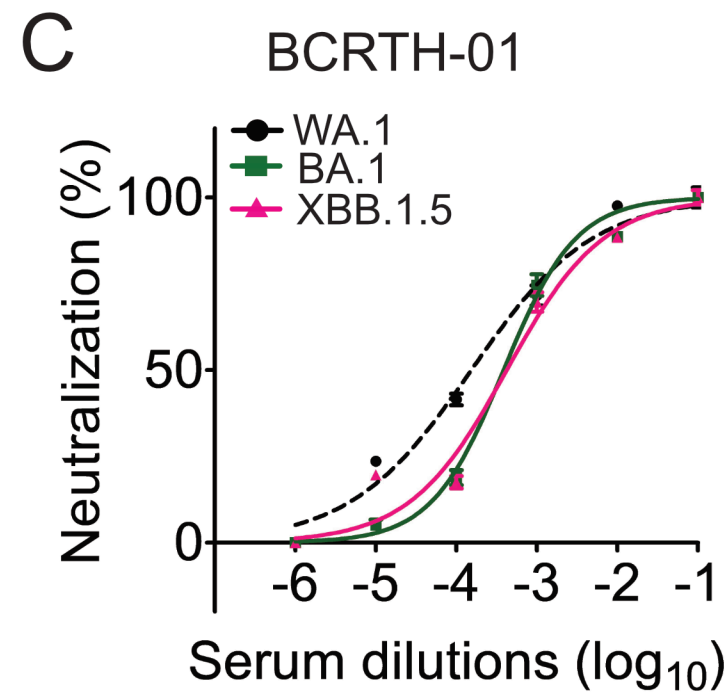

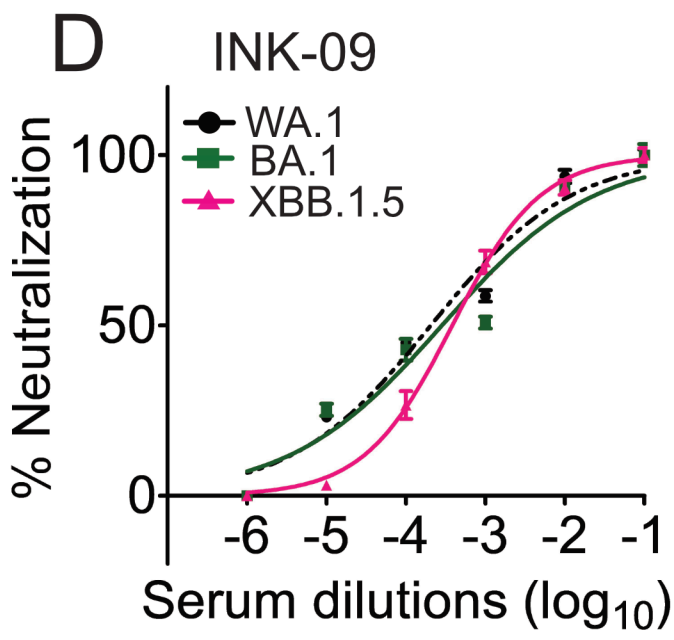

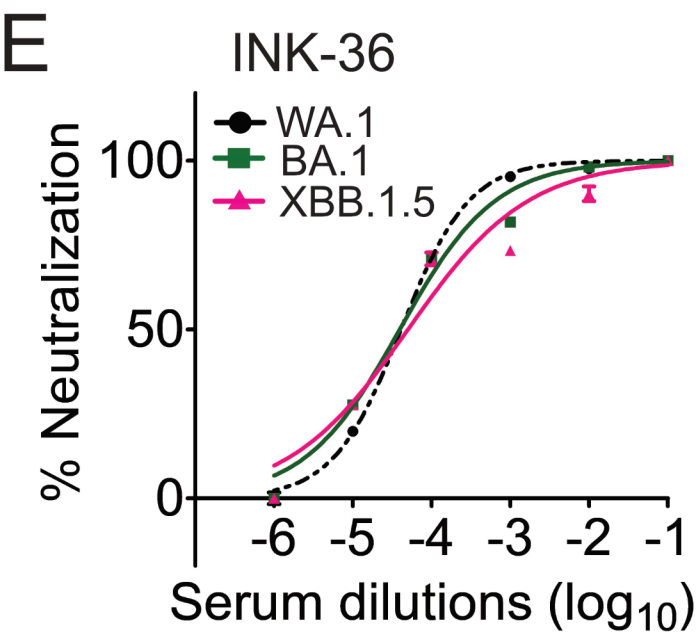

F

		Omicron	
Serum	WA.1	BA.1	XBB.1.5
BCRTH-01	1.00	0.40	0.36
INK-09	1.00	0.73	0.54
INK-36	1.00	1.04	0.82

1.00 0.36

Figure 5

Early 2022 breakthrough infection sera from India target the conserved cryptic class 5 epitope to counteract immune escape by SARS-CoV-2 variants

Indrani Das Jana[1], Kawkab Kanjo[2], Subhanita Roy[1], Munmun Bhasin[2], Shatarupa Bhattacharya[5], Indranath Banerjee[3], Subhasis Jana[6], Arjun Chatterjee[7], Alok Chakraborty[8], Suman Chakraborty[4], Budhaditya Mukherjee[5], Raghavan Varadarajan[2*], Arindam Mondal[1*]

[1]Department of Bioscience and Biotechnology, Indian Institute of Technology Kharagpur, Kharagpur-721302, India
[2]Molecular Biophysics Unit (MBU), Indian Institute of Science, Bengaluru-560012, India
[3]B.C. Roy Technology Hospital, Indian Institute of Technology Kharagpur, Kharagpur-721302, India
[4]Department of Mechanical Engineering, Indian Institute of Technology Kharagpur, Kharagpur-721302, India
[5]School of Medical Science and Technology, Indian Institute of Technology Kharagpur, Kharagpur-721302, India
[6]Purba Medinipur District Hospital, *Tamluk-721636*, India
[7]Institute of Neuroscience, *Kolkata*-700017
[8]ICMR-National Institute of Cholera and Enteric Diseases, Kolkata-700010, India

Correspondence*: varadar@iisc.ac.in (R.V.), arindam.mondal@iitkgp.ac.in (A.M.)

39 **Supplementary information**

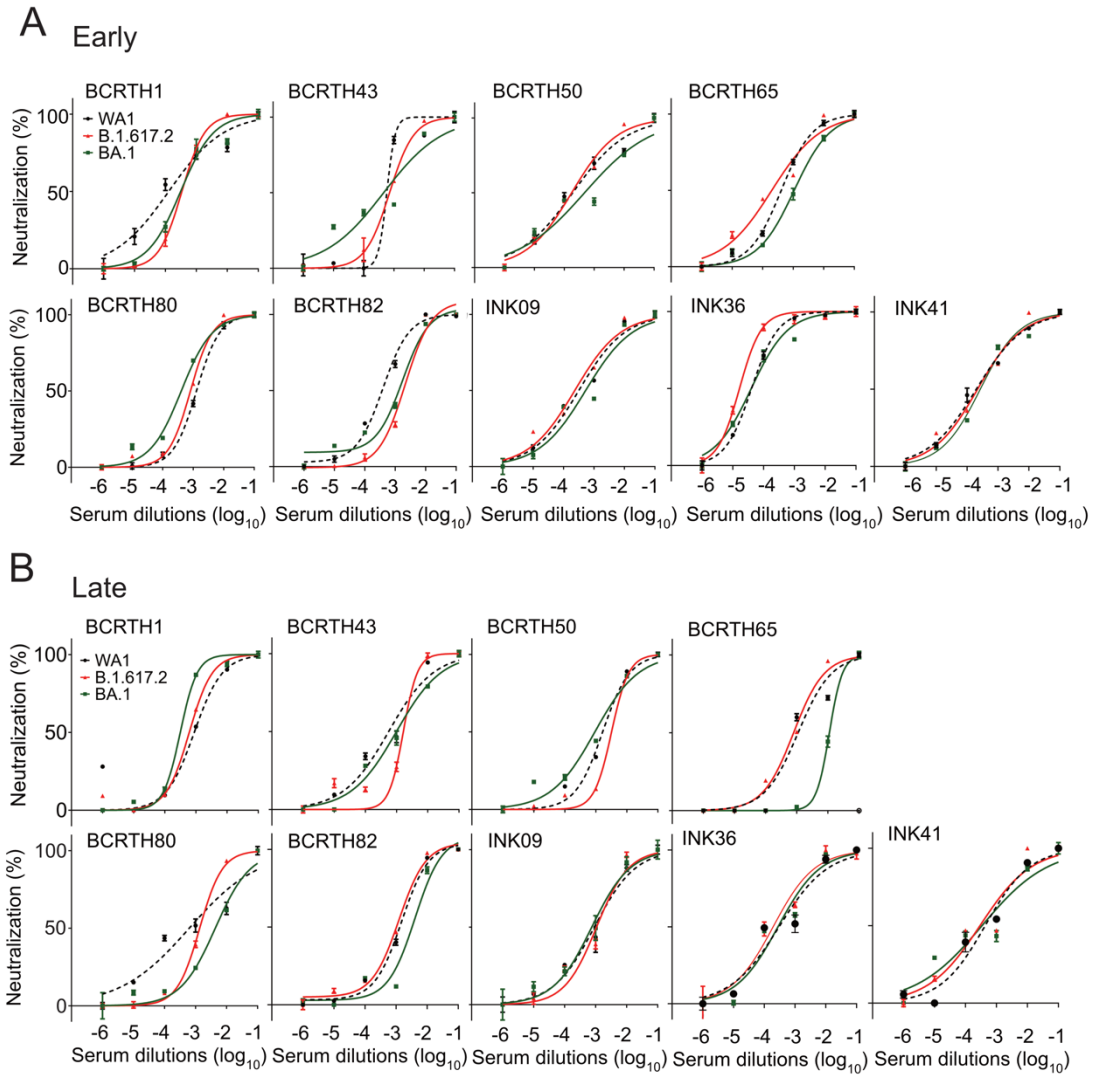

40

41 **Figure S1. Neutralizing activity of serum samples collected at early and late time points.**
42 Neutralization of the WA.1, B.1.617.2 and BA.1 pseudoviruses with nine serum samples collected
43 from the shortlisted volunteers during 1st and 2nd batches of sample collections, designated as (A)
44 early and (B) late time points.

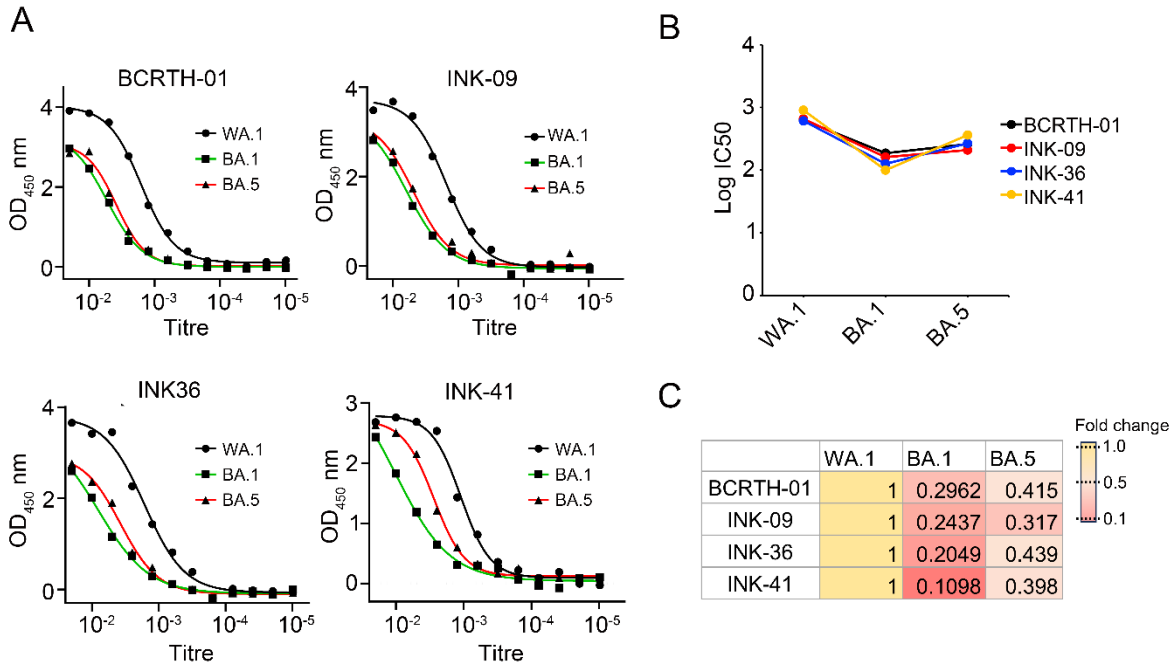

	WA.1	BA.1	BA.5
BCRTH-01	1	0.2962	0.415
INK-09	1	0.2437	0.317
INK-36	1	0.2049	0.439
INK-41	1	0.1098	0.398

Figure S2. The serum samples show high binding affinity towards spike RBD. (A) ELISA was performed to determine the binding affinity of the polyclonal serum samples towards spike RBD derived from WA.1 and Omicron subvariants BA.1 and BA.5. (B) Comparison between different serum samples in terms of their binding affinity towards different RBD variants. (C) Showing fold change in IC50 values for the BA.1 and BA.5 variants with respect to the WA.1.

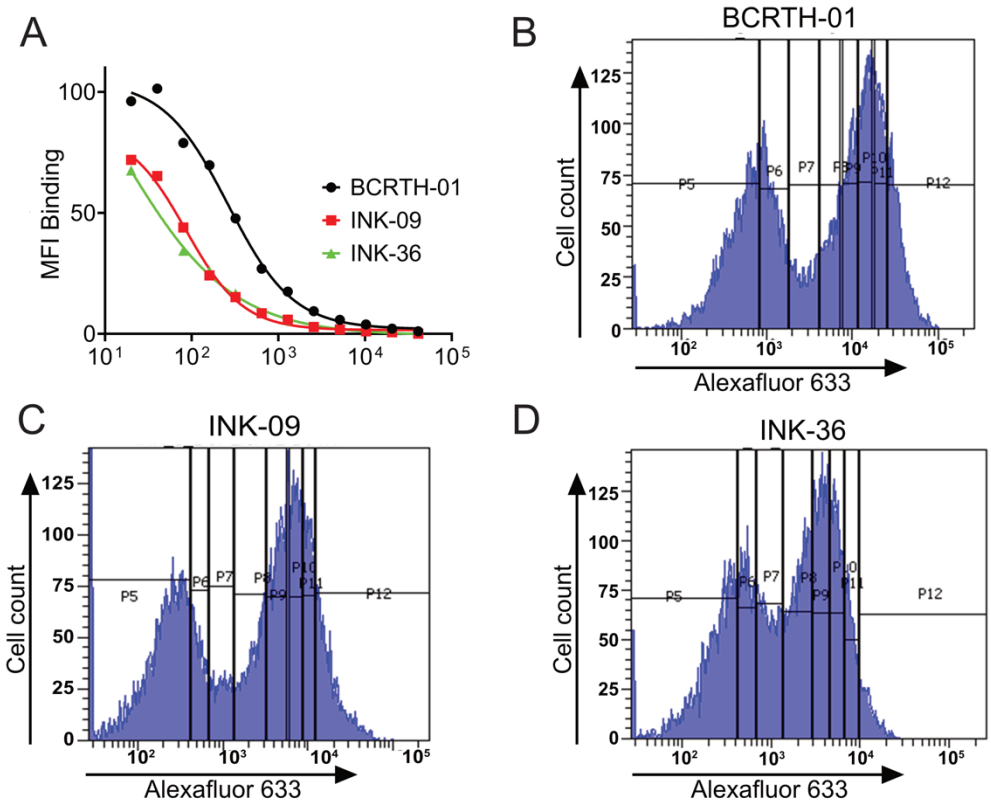

Figure S3. (A) The binding profile of the shortlisted serum samples to wild type RBD displayed on the yeast surface. (B, C and D) Histograms showing yeast cells binding to the indicated serum samples,

were sorted into eight gates based upon low to high binding affinity and the frequency of each variant's barcode in individual gates was determined by Illumina sequencing.

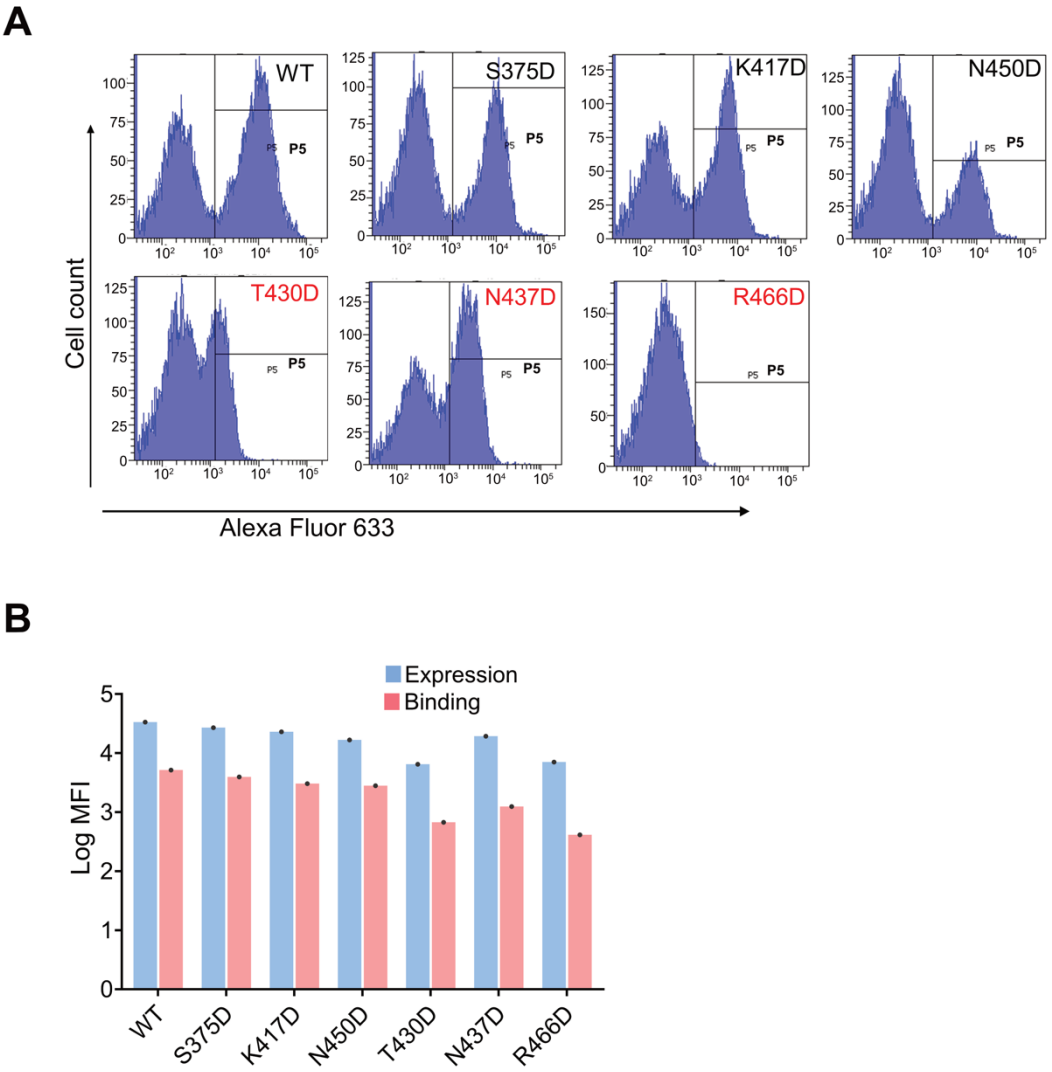

Figure S4. Validation of epitope and non-epitope residues identified by deep sequencing analysis. (A) The validation was carried out using FACS by quantifying the binding of WT and the selected RBD mutants to BCRTH-01 serum (B) MFI-Expression and MFI-binding of WT and mutant RBDs, harbouring mutations at the epitope and non-epitope residues are presented individually.

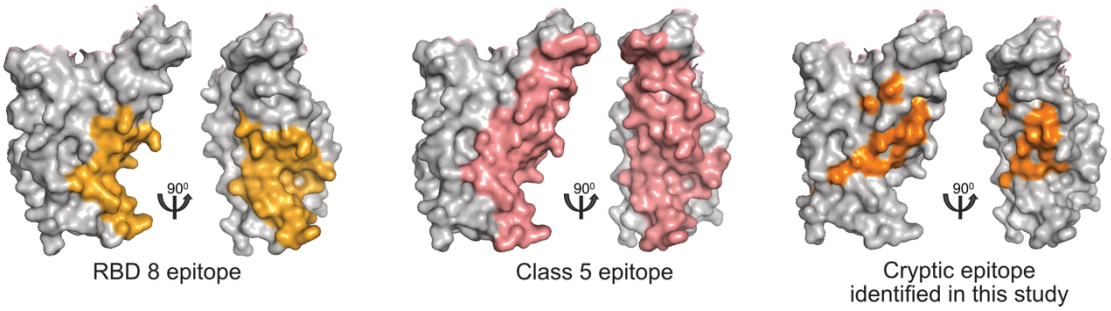

Figure S5: Surface representation of the RBD structure (PDB ID: 6M0J) with specific epitope residues color coded based on their classification. Epitope residues of RBD8 (colored in yellow), class 5 (colored in pale pink) and the rare cryptic epitope identified in this study (colored in orange) are individually depicted with separate colors.

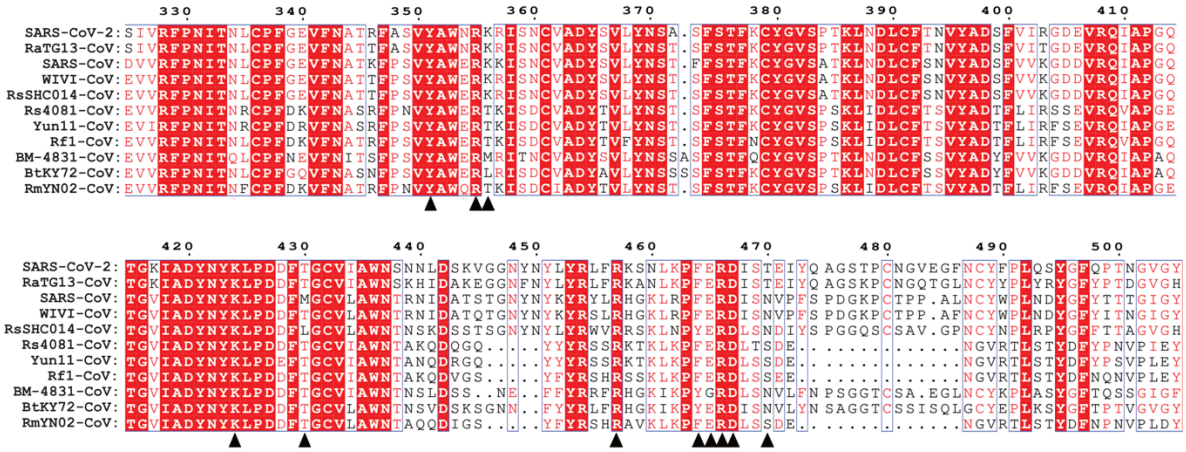

Figure S6. Multiple sequence alignment of different sarbecovirus spike RBD sequences. Black triangles mark the Class5/ RBD epitope residues.

Table S1. Classification of epitopes.

Residue No.	Epitopes for serum samples			Epitope class	Antibody	Reference
	BCRTH -01	INK -09	INK -36			
351	+	+	+	Class 5/ RBD8	N-612-056; BIOLS56/ IMCAS74/ WRAIR-2057/ WRAIR-2134	42–44,78
355	+	+	+	Class 5/ RBD8	N-612-056/ BIOLS56/ IMCAS74/ WRAIR-2063/ S2H97/ FD20/WRAIR-2057/WRAIR-2134	27,42–44,78,84,85
356	+	-	-	Class3/ Class 5/ RBD8	S309/ N-612-056/ IMCAS74/ WRAIR-2134	22,42–44
359	-	-	+	Class3	S309	22
364	+	-	-	Unclassified	-	-
380	-	+	+	Class4	COVA1-16, CR3022	25,86
381	+	-	-	Class4	COVA1-16, CR3022	25,86
387	+	-	-	Unclassified		-
403	+	+	+	Class1	C002, C102, C121	21
416	+	+	+	Class1/ Class4	C105, COVA1-16, C118, C022,	25,26,87
420	+	-	+	Class1	C105, LY-CoV-016	38,79,87
421	+	+	+	Class1	C102	21
424	-	+	+	Class 5/ RBD8	BIOLS56/ IMCAS74/ WRAIR-2057/ WRAIR-2134	43,44
430	+	-	-	Class4/ Class 5/ RBD8	C022/ BIOLS56/ IMCAS74/ WRAIR-2057/ WRAIR-2134	26,43,44
437	+	+	+	Class 4	C118	26
452	-	-	+	Class2	C144, C002	21
456	+	+	+	Class1	C002, C102, C121	21
457	+	+	-	Class 5	N-612-056, 6D6; WRAIR-2057/WRAIR-2134	42,44

464	+	+	+	Class 5/ RBD8	N-612-056/ 6D6 & 7D6/ BIOLS56/ IMCAS74/ WRAIR-2063/ S2H97/ WRAIR-2057/ WRAIR-2134	[27,42–44,78,84,85]
465	+	-	+	Class 5/ RBD8	N-612-056/ 6D6 & 7D6/ BIOLS56/ IMCAS74/ WRAIR-2063/ S2H97/ WRAIR-2057/ WRAIR-2134	[27,42–44,78,85]
466	+	+	+	Class 5/ RBD8	N-612-056/ 6D6 & 7D6/ BIOLS56/ IMCAS74/ WRAIR-2063/ S2H97/ WRAIR-2057/ WRAIR-2134	[42,43,78]
467	+	+	+	Class 5/ RBD8	N-612-056; IMCAS74/ WRAIR-2063/ S2H97/ WRAIR-2057/ WRAIR-2134	[42,43]
470	+	-	+	Class2/ Class 5/ RBD8	C144/ 7D6, 6D6/ WRAIR-2057	[21,78]
473	+	+	+	Class1	C102	[21]
475	-	-	+	Class1	C102	[21]
489	-	+	+	Class1	C102	[21]

Table S2. MFI ratios for the potential epitope residues

Sl No.	Residue	MFI-expression/ MFI-binding		
		BCRTH-01	**INK-09**	**INK-36**
1	351	1.295788	1.273718	1.157062
2	355	1.219729	1.239262	1.197349
3	356	1.17089	-	-
4	359	-	-	1.081459
5	364	1.182295	-	-
6	380	-	1.148814	1.077429
7	381	1.260786	-	-
8	387	1.230637	-	-
9	403	1.292267	1.172926	1.120017
10	416	1.329536	1.175896	1.101252
11	420	1.163761	-	1.072276
12	421	1.218064	1.168982	1.115263
13	424	-	1.192174	1.081695
14	430	1.270088	-	-
15	437	1.301646	1.107961	1.117455
16	452	-	-	1.076026
17	456	1.185845	1.252503	1.192579
18	457	1.225249	1.222689	-

19	464	1.246659	1.128143	1.087599
20	465	1.225858	-	1.080284
21	466	1.341557	1.187018	1.116536
22	467	1.242733	1.221766	1.118558
23	470	1.178698	-	1.063863
24	473	1.169721	1.145745	1.100281
25	475	-	-	1.102217
26	489	-	1.234014	1.144957